THE UNIVERSITY OF WARWICK

Original citation:
Burke, Siobhan, Ortner, Christoph and Süli, Endre. (2010) An adaptive finite element approximation of a variational model of brittle fracture. SIAM Journal on Numerical Analysis, Vol.48 (No.3). pp. 980-1012.

Permanent WRAP url:
http://wrap.warwick.ac.uk/43803

Copyright and reuse:
The Warwick Research Archive Portal (WRAP) makes this work of researchers of the University of Warwick available open access under the following conditions. Copyright © and all moral rights to the version of the paper presented here belong to the individual author(s) and/or other copyright owners. To the extent reasonable and practicable the material made available in WRAP has been checked for eligibility before being made available.

Copies of full items can be used for personal research or study, educational, or not-for-profit purposes without prior permission or charge. Provided that the authors, title and full bibliographic details are credited, a hyperlink and/or URL is given for the original metadata page and the content is not changed in any way.

Publisher's statement:
© SIAM
http://dx.doi.org/10.1137/080741033

A note on versions:
The version presented in WRAP is the published version or, version of record, and may be cited as it appears here.

For more information, please contact the WRAP Team at: publications@warwick.ac.uk

warwickpublicationswrap
highlight your research

http://wrap.warwick.ac.uk/

SIAM J. NUMER. ANAL.
Vol. 48, No. 3, pp. 980–1012
© 2010 Society for Industrial and Applied Mathematics

AN ADAPTIVE FINITE ELEMENT APPROXIMATION OF A VARIATIONAL MODEL OF BRITTLE FRACTURE*

SIOBHAN BURKE†, CHRISTOPH ORTNER†, AND ENDRE SÜLI†

Abstract. The energy of the Francfort–Marigo model of brittle fracture can be approximated, in the sense of Γ-convergence, by the Ambrosio–Tortorelli functional. In this work, we formulate and analyze two adaptive finite element algorithms for the computation of its (local) minimizers. For each algorithm, we combine a Newton-type method with residual-driven adaptive mesh refinement. We present two theoretical results which demonstrate convergence of our algorithms to local minimizers of the Ambrosio–Tortorelli functional.

Key words. adaptive finite element method, brittle fracture, free-discontinuity problem, Ambrosio–Tortorelli functional

AMS subject classifications. 65N30, 65N50, 74R10

DOI. 10.1137/080741033

1. Introduction.

Beginning with the work of Francfort and Marigo [25], a variational approach to the theory of quasi-static brittle fracture mechanics has experienced rapid and successful development. Upon recasting Griffith's idea of balancing energy release rate with a fictitious surface energy [27] as an energy minimization problem, Francfort and Marigo were able to formulate a model that was free of the usual constraints of fracture mechanics such as a predefined and piecewise smooth crack path. With the help of the theory of free-discontinuity problems [3], this model was soon shown to be well-posed in a surprisingly general setting [18, 19, 24]. We briefly review the model in section 1.1.

The model of Francfort and Marigo is posed in terms of the minimization of a highly irregular energy functional, which also occurs in image segmentation where it is known as the Mumford–Shah functional [30]. Several methods have been proposed in the literature, which regularize this energy in order to render the problem accessible to numerical simulation [10, 16, 31]. Such methods typically use the theory of Γ-convergence [12] to construct approximating functionals whose minimizers converge to those of the original functional.

In our experience, the Ambrosio–Tortorelli approximation [4, 5] is one of the most promising approaches. A particularly nice feature of the Ambrosio–Tortorelli functional is that its minimization can be reduced to the solution of elliptic boundary value problems that are straightforward to discretize, for example, by a finite element method. This approach has been used successfully by Bourdin, Francfort, and Marigo [11] and Bourdin [8, 9] for the simulation of problems that are usually inaccessible to traditional methods. A brief review of the Ambrosio–Tortorelli approximation is given in section 1.2.

The Ambrosio–Tortorelli approximation can be understood as a phase-field model for the crack set. To resolve the phase-field variable, the mesh near the crack has

*Received by the editors November 17, 2008; accepted for publication (in revised form) April 26, 2010; published electronically July 1, 2010. This work was supported by the EPSRC research programme *New Frontiers in the Mathematics of Solids* (OxMOS).
http://www.siam.org/journals/sinum/48-3/74103.html
†Mathematical Institute, University of Oxford, Oxford OX1 3LB, United Kingdom (burke@maths.ox.ac.uk, ortner@maths.ox.ac.uk, suli@maths.ox.ac.uk).

Copyright © by SIAM. Unauthorized reproduction of this article is prohibited.

to be significantly finer than the mesh that would be required to resolve the elastic deformation. Since we do not know the crack path in advance, it is therefore a natural idea to use an adaptively refined mesh. Using established techniques of adaptive finite element theory [36], we derive a residual estimate for the gradient of the Ambrosio–Tortorelli functional (see section 3.1). In section 3.2, we formulate two adaptive algorithms for which we use the residual estimates to steer the mesh refinement. In section 4, we prove that the second of these algorithms converges to a critical point of the Ambrosio–Tortorelli functional. We also prove that the first algorithm converges to a critical point under the assumption that the associated residuals converge to zero.

We conclude with an implementation of the adaptive algorithms for two computational examples in section 5.

In order to lay out the main ideas, our analysis in the present work is restricted to linearized elasticity in antiplane deformation and to linear finite elements. We will extend our results to more general approximations and a wider range of models in future work.

1.1. The Francfort–Marigo model of brittle fracture. In order to introduce the Francfort–Marigo model of brittle fracture, we briefly define the space of *special functions of bounded variation* [3, 22]. A knowledge of this space is not necessary for the main ideas contained in the paper.

For $p \in [1, \infty]$ and Ω an open domain in $\mathbb{R}^N$, we use $\mathrm{L}^p(\Omega)$ to denote the standard Lebesgue spaces on Ω and $\mathrm{H}^1(\Omega)$ to denote the standard Hilbertian Sobolev space on Ω. The N-dimensional Lebesgue and Hausdorff measures are denoted by $\mathcal{L}^N$ and $\mathcal{H}^N$, respectively.

We say that a function $f \in \mathrm{L}^1(\Omega)$ has bounded variation if

$$\sup \left\{ \int_\Omega f \mathrm{div} \varphi \, \mathrm{d}x \, : \varphi \in \mathrm{C}_0^1(\Omega; \mathbb{R}^N), \, |\varphi| \leq 1 \right\} < \infty.$$

The space of functions of bounded variation is denoted $\mathrm{BV}(\Omega)$. A function of bounded variation can exhibit discontinuities that are reflected in its distributional gradient. Given a function $f \in \mathrm{BV}(\Omega)$, the distributional derivative of f, denoted Df, is a Radon measure, which can be decomposed as

$$Df = \nabla f \mathcal{L}^N + (f^+(x) - f^-(x)) \otimes \nu_f(x) \mathcal{H}^{N-1} \lfloor J(f) + D^c f,$$

where ∇f is called the *approximate gradient* of f, $J(f)$ is the *jump set* of f, ν_f is the *unit normal* to $J(f)$, $f^\pm$ are the *inner and outer traces* of f on $J(u)$ with respect to ν_f, and $D^c f$ is called the *Cantor part* of the derivative. We refer the reader to [3] for the precise definitions of these terms. The space of special functions of bounded variation is then defined as

$$\mathrm{SBV}(\Omega) := \{ f \in \mathrm{BV}(\Omega) : D^c f = 0 \}.$$

We are now in a position to describe the Francfort–Marigo model of brittle fracture [25]. The crack-free reference configuration of a linearly elastic body is denoted by Ω. The set Ω is taken to be an open, bounded, and connected domain with Lipschitz boundary $\partial\Omega$ (we shall relax this assumption later).

For each $u \in \mathrm{SBV}(\Omega)$ and for each Hausdorff measurable set Γ, we define the

Copyright © by SIAM. Unauthorized reproduction of this article is prohibited.

bulk, surface, and total energy, respectively, by

$$E_B(u) := \int_{\Omega\setminus J(u)} |\nabla u|^2 \,\mathrm{d}x, \tag{1.1}$$

$$E_S(\Gamma) := \kappa \mathcal{H}^{N-1}(\Gamma), \quad \text{and} \tag{1.2}$$

$$E(u,\Gamma) := \begin{cases} E_B(u) + E_S(\Gamma) & \text{if } \mathcal{H}^{N-1}(J(u)\setminus\Gamma) = 0, \\ +\infty & \text{otherwise.} \end{cases} \tag{1.3}$$

The energy functional $E(u,\Gamma)$ reflects Griffith's principle that, to create a crack, one has to *spend* an amount of elastic energy that is proportional to the area of the crack created [27]. The constant of proportionality κ is called *fracture toughness* and is often also denoted G_c (critical energy release rate). The crack set Γ and the jump set $J(u)$ are decoupled in the definition of the total energy in order to be able to impose irreversibility of the crack evolution. The quasi-static evolution will be obtained upon minimizing E subject to several constraints, which we introduce momentarily.

We wish to study how the body evolves in time under the action of a varying load $g(t)$, which is applied on an open subset $\Omega_D \subset \Omega$ of positive N-dimensional Lebesgue measure. We assume that $g \in \mathrm{L}^\infty(0,T;\mathrm{W}^{1,\infty}(\Omega)) \cap \mathrm{W}^{1,1}(0,T;\mathrm{H}^1(\Omega))$, and we define

$$\mathcal{A}(g(t)) := \big\{u \in \mathrm{SBV}(\Omega) : u|_{\Omega_D} = g(t)|_{\Omega_D}\big\}.$$

The fact that the Dirichlet condition is imposed on a set of positive N-dimensional Lebesgue measure is mostly technical and ensures that the jump set on the *Dirichlet boundary* $\partial\Omega_D \cap \Omega$ is well defined. Since we work in antiplane deformation, the boundary displacement is applied in a direction perpendicular to the plane in which the initial configuration of the domain lies. We call $\partial\Omega_N := \partial\Omega\setminus\partial\Omega_D$ the *Neumann boundary*.

It is most intuitive to introduce the Francfort–Marigo model through a time discretization. Let $0 = t_0 < t_1 < \cdots < t_F = T$ be a discretization of the time interval $[0,T]$, with $\Delta t := \max\{t_k - t_{k-1} : k = 1,\dots,F\}$. Given an initial crack $\Gamma(0)$ (which should be the jump set of an SBV function $u(0)$), we seek $(u(t_k),\Gamma(t_k))$, $k = 1,\dots,F$, such that the following properties hold:

1. *irreversibility:* $\Gamma(t_k) \supset \Gamma(t_{k-1})$;
2. *global stability:* $E(u(t_k),\Gamma(t_k)) \le E(v,\Gamma)$ for all $v \in \mathcal{A}(g(t_k))$ and $\Gamma \supset \Gamma(t_{k-1})$.

In practice, this formulation requires the successive solution of the global minimization problems

$$u(t_k) := \operatorname*{argmin}_{v\in\mathcal{A}(g(t_k))} E_B(v) + E_S(J(v)\cup\Gamma(t_{k-1})), \quad \Gamma(t_k) := J(u(t_k))\cup\Gamma(t_{k-1}). \tag{1.4}$$

In this formulation, the problem is accessible to the direct method of the calculus of variations to prove the existence of solutions to the time-discrete Francfort–Marigo model [1, 2, 3, 20].

It remains to describe the limit of the time-discrete evolution as $\Delta t \to 0$. In full generality, it was first shown by Francfort and Larsen [24] (an earlier result is due to Dal Maso and Toader [19] and the extension to finite elasticity was developed by Dal Maso, Francfort, and Toader [18]) that it is indeed possible to extract weakly convergent subsequences of the discrete solutions and thus prove the existence of a trajectory $u \in \mathrm{BV}(0,T;\mathrm{SBV}(\Omega))$ with crack set $\Gamma(t) = \cup_{s<t} J(u(s))$, $t \in (0,T]$, such that the following properties hold:

Copyright © by SIAM. Unauthorized reproduction of this article is prohibited.

1. *irreversibility:* $\Gamma(s) \subset \Gamma(t)$ for all $s, t \in [0, T]$ such that $s \le t$;
2. *global stability:* $E(u(t), \Gamma(t)) \le E(v, J(v) \cup \Gamma(t))$ for all $v \in \mathcal{A}(g(t))$;
3. *energy balance:* $E(u(t), \Gamma(t)) - E(u(s), \Gamma(s)) = 2 \int_s^t \int_\Omega \nabla u(\tau) \cdot \nabla \dot{g}(\tau) \, \mathrm{d}x \, \mathrm{d}\tau$.

These three conditions should not be taken as the definition of a quasi-static crack evolution, as they underconstrain the system; however, they demonstrate that the limits of the time-discrete version of the model have several important properties, namely unilateral global stability and energy conservation.

The ability to predict complicated crack paths is the greatest strength of the Francfort–Marigo model and the reason for its popularity. In other respects, it may fall short of physical reality even on a qualitative level. For example, Francfort and Marigo acknowledged in their seminal work [25] that, from a mechanical point of view, it would be preferable to define an evolution by means of local minimizers. Unfortunately, this has proven to be a major challenge, which has not been resolved. In our numerical methods, which we describe in sections 2–5, we will be pragmatic regarding this point and will not make the distinction between local and global minimizers. In fact, we are unaware of an existing method that is able to compute global minimizers of highly nonconvex functionals such as the Ambrosio–Tortorelli approximation, which we introduce next.

1.2. The Ambrosio–Tortorelli approximation. Obtaining a numerical approximation of the time-discrete Francfort–Marigo model is a nontrivial task. A direct discretization of the minimization problem (1.4) poses difficulties due to the irregularity of the energy functional and the need to accurately measure the surface area of the crack. A successful approach is to work instead with a regularization of $E(u, \Gamma)$, which is able to represent the crack set in a manner more readily tractable by numerical methods. The regularized functional is chosen to approximate $E(u, \Gamma)$ in the sense of Γ-convergence [12]. Consequently, minimizers of the approximating functional converge to minimizers of $E(u, \Gamma)$ together with convergence of the minimized energy.

One such approximation of $E(u, \Gamma)$ is the Ambrosio–Tortorelli functional $I_\varepsilon : \mathrm{H}^1(\Omega; \mathbb{R}) \times \mathrm{H}^1(\Omega; [0, 1]) \to \mathbb{R}$, defined for $0 < \eta \ll \varepsilon \ll 1$ as follows:

$$I_\varepsilon(u, v) := \int_\Omega (v^2 + \eta) |\nabla u|^2 \, \mathrm{d}x + \kappa \int_\Omega \left[\frac{1}{4\varepsilon} (1 - v)^2 + \varepsilon |\nabla v|^2 \right] \mathrm{d}x. \tag{1.5}$$

The family of functionals $\{I_\varepsilon\}_{\varepsilon > 0}$ satisfies the following Γ-convergence result [11].

Let us define

$$G_\varepsilon(\hat{u}, \hat{v}) := \begin{cases} I_\varepsilon(\hat{u}, \hat{v}) & \text{if } \hat{u} \in \mathrm{H}^1(\Omega),\ \hat{u} = g(t) \text{ on } \Omega_D,\ \hat{v} \in \mathrm{H}^1(\Omega; [0, 1]), \\ +\infty & \text{otherwise,} \end{cases}$$

$$G(\hat{u}, \hat{v}) := \begin{cases} E(\hat{u}, J(\hat{u})) & \text{if } \hat{u} \in \mathcal{A}(g(t)),\ \hat{v} = 1 \text{ a.e. on } \Omega, \\ +\infty & \text{otherwise;} \end{cases}$$

then G_ε Γ-converges to G in $\mathrm{L}^1(\Omega) \times \mathrm{L}^1(\Omega)$ as $\varepsilon \to 0$.

This is a modification of the original Ambrosio–Tortorelli Γ-convergence result [4] for the approximation of the Mumford–Shah functional [30]. The existence of minimizers to I_ε has been shown in [5] for each ε, $\eta > 0$. Further generalizations of the Γ-convergence result have since been established in [7, 23].

Using the Ambrosio–Tortorelli functional, an approximation to the time-discrete Francfort–Marigo model can be computed as follows. At time $t = t_0$, find

$$(u_\varepsilon(t_0), v_\varepsilon(t_0)) \in \operatorname{argmin}\{I_\varepsilon(\hat{u}, \hat{v}) : \hat{u} \in \mathrm{H}^1(\Omega),\ \hat{u} = g(t_0) \text{ on } \Omega_D;\ \hat{v} \in \mathrm{H}^1(\Omega; [0, 1])\}.$$

Copyright © by SIAM. Unauthorized reproduction of this article is prohibited.

At subsequent times $t = t_k$, $k = 1, \dots, F$, find $(u_\varepsilon(t_k), v_\varepsilon(t_k))$ satisfying

$$(u_\varepsilon(t_k), v_\varepsilon(t_k)) \in \operatorname{argmin}\{I_\varepsilon(\hat{u}, \hat{v}) : \hat{u} \in \mathrm{H}^1(\Omega), \quad \hat{u} = g(t_k) \text{ on } \Omega_D;\ \hat{v} \in \mathrm{H}^1(\Omega), \hat{v} \le v_\varepsilon(t_{k-1})\}. \tag{1.6}$$

At the fixed time $t = t_k$, the function $u_\varepsilon(t_k)$ is an approximation of the displacement of the body $u(t_k)$, with $u_\varepsilon(t_k) \to u(t_k)$ in $\mathrm{L}^1(\Omega)$ as $\varepsilon \to 0$. The auxiliary function $v_\varepsilon(t_k)$ is introduced in order to represent the crack $\Gamma(t_k)$. A truncation argument shows that

$$0 \le v_\varepsilon(x, t_k) \le 1 \qquad \text{a.e. } x \in \Omega.$$

The crack is then approximated by the subset of the domain on which $v_\varepsilon(t_k)$ takes values close to zero. Conversely, the unfractured part of the body is represented by the subset of the domain on which $v_\varepsilon(t_k)$ takes values close to one. The transition layer between the two regimes has thickness of order ε. In the limit $\varepsilon \to 0$, the minimization of I_ε requires that $v_\varepsilon(t_k) \to 1$ a.e. Consequently, the transition layer becomes infinitely thin, with $v_\varepsilon(t_k) \to 0$ only on the $(N-1)$-dimensional surface representing the crack.

It was shown by Giacomini [26] that an evolution satisfying (1.6) converges as $\Delta t, \varepsilon \to 0$ to an evolution satisfying the conditions of the time-continuous Francfort–Marigo model. We will therefore restrict our consideration to the problem of minimizing the Ambrosio–Tortorelli functional at the fixed moment in time $t = t_k$ and for fixed values of ε and η.

The condition $\hat{v} \le v_\varepsilon(t_{k-1})$ in (1.6) enforces the irreversibility of the crack [26]. In practice, however, we choose to implement the irreversibility criterion through the following equality constraint introduced by Bourdin [8]. If at time $t = t_{k-1}$, $k \in \{1, \dots, F\}$, the set

$$\mathtt{CR}(t_{k-1}) := \{x \in \overline{\Omega} : v_\varepsilon(x, t_{k-1}) < \mathtt{CRTOL}\} \tag{1.7}$$

is nonempty for some small specified tolerance CRTOL, then fix

$$v_\varepsilon(x, t_i) = 0 \qquad \forall x \in \mathtt{CR}(t_{k-1}) \text{ and } \forall i \text{ such that } k \le i \le F.$$

Thus, if, at a particular time $t = t_{k-1}$, $v_\varepsilon(x, t_{k-1})$ is close enough to zero to indicate that the point x lies on the crack path, then v_ε is set to be zero at that point for all subsequent time steps. This simplifies the minimization over $\hat{v}$ by allowing the use of an unconstrained minimization algorithm.

Remark 1. We note that this modification of the irreversibility criterion could result in a crack-widening effect, since it is conceivable that setting $v_\varepsilon(x, t_{k-1})$ to zero causes v_ε to be pulled below CRTOL at points in a neighborhood of x, which will then be set to zero at $t = t_k$. In practice, however, we do not observe this effect to occur in the discrete case. As such, we continue to use this formulation of irreversibility here and refer the reader to [14] for an alternative implementation that uses a modified monotonicity condition.

A numerical discretization of this minimization problem has been proposed and implemented by Bourdin, Francfort, and Marigo [11] and Bourdin [8, 9] in which a finite element method is used in conjunction with a minimization algorithm to compute minimizers of the Ambrosio–Tortorelli functional. The method uses a fine mesh to discretize the whole domain. It does, however, seem apparent to us that the

Copyright © by SIAM. Unauthorized reproduction of this article is prohibited.

behavior of minimizers can be sufficiently resolved using a mesh that is fine only in a layer around the crack, whilst remaining relatively coarse elsewhere. Naturally, we do not know the location of the crack a priori. Thus, we propose using an adaptive finite element method for the numerical computation of minimizers.

One could argue that the refinement of only part of the mesh causes the crack to favor growth in this direction; we believe, however, that a carefully designed adaptive algorithm can circumvent this eventuality. We refer the reader to Remark 5 for a further discussion of this point.

1.3. Critical points. In the Ambrosio–Tortorelli model, Lipschitz regularity of the domain is not required. Since, in practice, it is more convenient to model a pre-existing crack by a slit domain rather than an initial crack field v_0, we will, from now on, drop the assumption that Ω is a Lipschitz domain. Motivated by the fact that we will need to partition Ω for the purpose of defining a finite element approximation, we shall assume that Ω is a polyhedral domain. By this, we simply mean that Ω possesses a finite partition into nondegenerate N-simplexes: *there exist open, disjoint, nondegenerate simplexes* $T_1, \dots, T_K \subset \Omega$ *such that* $\mathcal{L}^N(\Omega \setminus \cup_k T_k) = 0$ (see also section 2). In that case, it is clear that the usual trace and embedding theorems for Sobolev spaces hold on Ω.

Since we consider the minimization of the Ambrosio–Tortorelli functional at the fixed time $t = t_k$, it is useful to define the following function spaces:

$$\mathrm{H}^1_D(\Omega) := \{w \in \mathrm{H}^1(\Omega) \,:\, w = 0 \text{ on } \Omega_D\}, \tag{1.8}$$

$$\mathrm{H}^1_g(\Omega) := \{w \in \mathrm{H}^1(\Omega) \,:\, w = g(t_k) \text{ on } \Omega_D\}, \tag{1.9}$$

$$\mathrm{H}^1_c(\Omega) := \{w \in \mathrm{H}^1(\Omega) \,:\, w = 0 \text{ on } \mathtt{CR}(t_{k-1})\}. \tag{1.10}$$

We also fix ε and η, and for simplicity we set $\kappa = 1$. Accordingly we choose to relabel the Ambrosio–Tortorelli functional as $I : \mathrm{H}^1_g(\Omega) \times \mathrm{H}^1_c(\Omega) \to \mathbb{R} \cup \{+\infty\}$, where

$$I(u,v) := \int_\Omega \left[(v^2+\eta)|\nabla u|^2 + \alpha(1-v)^2 + \varepsilon|\nabla v|^2\right] \mathrm{d}x, \tag{1.11}$$

and $\alpha = 1/4\varepsilon$.

It can be seen, using a truncation argument, that any local minimizer (u,v) of I (in the $\mathrm{H}^1(\Omega) \times \mathrm{H}^1(\Omega)$ topology) satisfies $0 \le v(x) \le 1$ a.e. in Ω. Thus all relevant trial functions for v lie in the space $\mathrm{L}^\infty(\Omega)$. As such, in the following discussion of differentiability of I, we work with trial functions for v from the space $\mathrm{H}^1(\Omega) \cap \mathrm{L}^\infty(\Omega)$.

Proposition 1.1. *I is Fréchet-differentiable in* $\mathrm{H}^1(\Omega) \times (\mathrm{H}^1(\Omega) \cap \mathrm{L}^\infty(\Omega))$.

Proof. Let $(u,v) \in \mathrm{H}^1(\Omega) \times (\mathrm{H}^1(\Omega) \cap \mathrm{L}^\infty(\Omega))$. A straightforward calculation yields that the directional derivative of I at (u,v) in the direction $(\varphi,\psi) \in \mathrm{H}^1(\Omega) \times (\mathrm{H}^1(\Omega) \cap \mathrm{L}^\infty(\Omega))$ is given by

$$\begin{aligned} I'(u,v;\varphi,\psi) &= 2\int_\Omega (v^2+\eta)\nabla u \cdot \nabla\varphi \,\mathrm{d}x + 2\int_\Omega \left[v\psi|\nabla u|^2 + \alpha(v-1)\psi + \varepsilon\nabla v\cdot\nabla\psi\right] \mathrm{d}x \\ &=: 2a(v;u,\varphi) + 2b(u;v,\psi). \end{aligned}$$

This is in fact the Fréchet derivative, since

$$\begin{aligned} g(u,v;\varphi,\psi) &:= I(u+\varphi, v+\psi) - I(u,v) - I'(u,v;\varphi,\psi) \\ &= \int_\Omega [\psi^2|\nabla u|^2 + |\nabla\varphi|^2\big((v+\psi)^2+\eta\big) \\ &\qquad + (4v\psi + 2\psi^2)\nabla u\cdot\nabla\varphi + \alpha\psi^2 + \varepsilon|\nabla\psi|^2] \,\mathrm{d}x \end{aligned}$$

Copyright © by SIAM. Unauthorized reproduction of this article is prohibited.

satisfies

$$\begin{aligned}|g(u,v;\varphi,\psi)| \leq\ & \|\psi\|^2_{\mathrm{L}^\infty(\Omega)}\|\nabla u\|^2_{\mathrm{L}^2(\Omega)} + \|(v+\psi)^2+\eta\|_{\mathrm{L}^\infty(\Omega)}\|\nabla\varphi\|^2_{\mathrm{L}^2(\Omega)}\\ &+4\|v\|_{\mathrm{L}^\infty(\Omega)}\|\psi\|_{\mathrm{L}^\infty(\Omega)}\|\nabla u\|_{\mathrm{L}^2(\Omega)}\|\nabla\varphi\|_{\mathrm{L}^2(\Omega)}\\ &+2\|\psi\|^2_{\mathrm{L}^\infty(\Omega)}\|\nabla u\|_{\mathrm{L}^2(\Omega)}\|\nabla\varphi\|_{\mathrm{L}^2(\Omega)}\\ &+\alpha\|\psi\|^2_{\mathrm{L}^2(\Omega)}+\varepsilon\|\nabla\psi\|^2_{\mathrm{L}^2(\Omega)},\end{aligned}$$

and thus

$$\begin{aligned}&\frac{|g(u,v;\varphi,\psi)|}{\|\varphi\|_{\mathrm{H}^1(\Omega)}+\|\psi\|_{\mathrm{H}^1(\Omega)}+\|\psi\|_{\mathrm{L}^\infty(\Omega)}}\to 0\\ &\text{as }\ (\|\varphi\|_{\mathrm{H}^1(\Omega)}+\|\psi\|_{\mathrm{H}^1(\Omega)}+\|\psi\|_{\mathrm{L}^\infty(\Omega)})\ \to\ 0. \qquad \square\end{aligned}$$

Remark 2. We note that $I(u,v)$ is not finite for all $(u,v)\in \mathrm{H}^1(\Omega)\times\mathrm{H}^1(\Omega)$, and thus I is *not* Gâteaux-differentiable in $\mathrm{H}^1(\Omega)\times\mathrm{H}^1(\Omega)$. This motivates the following definition of a critical point.

DEFINITION 1.2. *We say that* $(u,v)\in \mathrm{H}^1_g(\Omega)\times(\mathrm{H}^1_c(\Omega)\cap\mathrm{L}^\infty(\Omega))$ *is a* critical point *of* I *if* $I'(u,v;\varphi,\psi)=0$ *for all* $\varphi\in\mathrm{H}^1_D(\Omega)$ *and* $\psi\in\mathrm{H}^1_c(\Omega)\cap\mathrm{L}^\infty(\Omega)$.

PROPOSITION 1.3. *If* $(u,v)\in \mathrm{H}^1_g(\Omega)\times(\mathrm{H}^1_c(\Omega)\cap\mathrm{L}^\infty(\Omega))$ *is a critical point of* I, *then* $0\leq v(x)\leq 1$ *for a.e.* $x\in\Omega$.

Proof. Suppose that (u,v) is a critical point of I and that there exist subsets A_1 and A_2 of Ω with $|A_1\cup A_2|>0$ such that $v>1$ on A_1 and $v<0$ on A_2. Since (u,v) is a critical point, it follows that

$$\int_\Omega \left[v\psi|\nabla u|^2+\alpha(v-1)\psi+\varepsilon\nabla v\cdot\nabla\psi\right]\,\mathrm{d}x=0\quad\forall\psi\in\mathrm{H}^1_c(\Omega)\cap\mathrm{L}^\infty(\Omega).$$

Choosing

$$\psi(x)=\begin{cases}1-v(x) & \text{if } x\in A_1,\\ 0 & \text{if } x\in\Omega\backslash(A_1\cup A_2),\\ -v(x) & \text{if } x\in A_2\end{cases}$$

yields

$$\int_{A_1}\left[v(1-v)|\nabla u|^2-\alpha(1-v)^2-\varepsilon|\nabla v|^2\right]\mathrm{d}x-\int_{A_2}\left[v^2|\nabla u|^2+\alpha v(v-1)+\varepsilon|\nabla v|^2\right]\mathrm{d}x=0,$$

which is a contradiction, since the left-hand side is strictly negative. $\square$

2. Finite element approximation and minimization.

2.1. Finite element discretization. Since we assumed that Ω is a polyhedral domain (see section 1.3), we may discretize it as follows. Let $\mathcal{T}_h$ be a subdivision of Ω into N-dimensional open simplexes $T\in\mathcal{T}_h$ such that $\overline{\Omega}=\cup_{T\in\mathcal{T}_h}\overline{T}$ and $T_i\cap T_j=\emptyset$ for T_i, $T_j\in\mathcal{T}_h$, with $i\neq j$. The subdivision $\mathcal{T}_h$ is chosen in such a way that the boundary of Ω_D is discretized as the union of faces of simplexes from $\mathcal{T}_h$.

We define $h:=\max_{T\in\mathcal{T}_h}\mathrm{diam}(T)$, and each simplex $T\in\mathcal{T}_h$ is taken to be an affine transformation of the open unit simplex

$$\hat{T}:=\{\hat{x}=(\hat{x}_1,\ldots,\hat{x}_N):0<\hat{x}_i,\ i=1,\ldots,N,\ 0<\hat{x}_1+\cdots+\hat{x}_N<1\}.$$

Each simplex $T\in\mathcal{T}_h$ is called an *element*. We assume that the subdivision is conforming; that is, the intersection of the closure of any two elements either is empty

Copyright © by SIAM. Unauthorized reproduction of this article is prohibited.

or is along an entire k-dimensional face, $0 \le k \le N-1$. We also require that the subdivision be shape regular, i.e.,

$$\sup_{T\in\mathcal{T}_h} \frac{h_T}{\rho_T} \le K$$

for some $K \in (0,\infty)$, where $h_T := \operatorname{diam}(T)$ and ρ_T is the diameter of the largest N-dimensional ball contained in T.

Let $N_h \subset \mathbb{N}$ denote an index set for the vertices of $\mathcal{T}_h$. For a vertex with index $i \in N_h$, let x_i denote the position of the vertex and let ζ_i be the continuous piecewise linear basis function such that $\zeta_i(x_j) = \delta_{ij}$. Define $N_{D,h} := \{i \in N_h : x_i \in \overline{\Omega}_D\}$.

Let $\mathcal{E}_h$ denote the set of $(N-1)$-dimensional open faces in the subdivision with $\mathcal{E}_{D,h} := \{e \in \mathcal{E}_h : e \subseteq \overline{\Omega}_D\}$, $\mathcal{E}_{N,h} := \{e \in \mathcal{E}_h : e \subseteq \partial\Omega_N\}$, and $\mathcal{E}_{I,h} := \{e \in \mathcal{E}_h \backslash (\mathcal{E}_{D,h} \cup \mathcal{E}_{N,h})\}$. We define E_h, $E_{D,h}$, $E_{N,h}$, and $E_{I,h}$ as the union of all faces in $\mathcal{E}_h$, $\mathcal{E}_{D,h}$, $\mathcal{E}_{N,h}$, and $\mathcal{E}_{I,h}$, respectively.

For all $i \in N_h$, let ω_i be the closure of the union of elements $T \in \mathcal{T}_h$ that have x_i as the position of a vertex, that is, $\omega_i := \operatorname{supp}(\zeta_i)$. For a face $e \in \mathcal{E}_h$ and element $T \in \mathcal{T}_h$, define $\omega_e := \cup_{i\in N_h : x_i \in \overline{e}} \omega_i$, $\omega_T := \cup_{i\in N_h : x_i \in \overline{T}} \omega_i$, and $h_e := \operatorname{diam}(e)$.

We now define the finite element spaces

$$X_h := \left\{ \sum_{i\in N_h} \lambda_i \zeta_i : \lambda_i \in \mathbb{R} \right\},$$

$$X_{h,D} := \left\{ \sum_{i\in N_h} \lambda_i \zeta_i : \lambda_i \in \mathbb{R},\ \lambda_i = 0\ \forall i \in N_{D,h} \right\}$$

and the finite element space at time $t = t_k$

$$X^k_{h,g} := \left\{ \sum_{i\in N_h} \lambda_i \zeta_i : \lambda_i \in \mathbb{R},\ \lambda_i = g(t_k, x_i)\ \forall i \in N_{D,h} \right\}.$$

In order to define a discrete function space setting for the phase-field variable v, we must first define the discrete analogue of $\mathrm{CR}(t_{k-1})$. For a given $v_h \in X_h$ and a small specified tolerance `CRTOL`, we define

$$\mathcal{E}^{\mathrm{CR}}_h(t_{k-1}) := \{e \in \mathcal{E}_h : v_h(x, t_{k-1}) \le \texttt{CRTOL}\ \forall x \in \overline{e}\} \quad \text{and} \quad \mathrm{CR}_h(t_{k-1}) := \bigcup_{e\in\mathcal{E}^{\mathrm{CR}}_h} \overline{e}.$$

We now define the finite element space

$$X^k_{h,c} := \{w_h \in X_h : w_h(x) = 0\ \forall x \in \mathrm{CR}_h(t_{k-1})\}.$$

Since we consider a fixed time t_k, we relabel $X^k_{h,g}$ and $X^k_{h,c}$ as $X_{h,g}$ and $X_{h,c}$, respectively, for ease of notation. Also, for simplicity, we assume throughout that g lies in the finite element space X_h.

For our subsequent analysis, we require the discrete formulation to satisfy a maximum principle analogous to Proposition 1.3. In order to accomplish this, we use a mass lumping approximation [35, Chapter 11] for I together with an assumption on the stiffness matrix, which can be achieved through typical mesh regularity conditions.

The mass lumping approximation of I is defined to be the functional

$$I_h(u_h, v_h) := \int_\Omega \left[\big(P_h(v_h^2) + \eta\big)|\nabla u_h|^2 + \alpha P_h\big((v_h - 1)^2\big) + \varepsilon|\nabla v_h|^2 \right] \mathrm{d}x, \tag{2.1}$$

where $P_h : \mathrm{C}(\overline{\Omega}) \mapsto X_h$ is the standard nodal interpolation operator [13, section 3.3].

Copyright © by SIAM. Unauthorized reproduction of this article is prohibited.

Let K be the $|N_h| \times |N_h|$ stiffness matrix with entries $(k_{ij})_{i,j \in N_h}$; then we assume that

$$k_{ij} := \int_\Omega \nabla \zeta_i \cdot \nabla \zeta_j \, \mathrm{d}x \leq 0 \qquad \forall i \neq j \in N_h. \tag{2.2}$$

This condition has been studied in detail in two dimensions [17], [34, p. 78] and three dimensions [28]. We note that this assumption is made only for technical purposes, and in practice we do not believe that it is necessary for ensuring that the conclusion of Proposition 2.2 holds; see Remark 7.

DEFINITION 2.1. *We say that* $(u_h, v_h) \in X_{h,g} \times X_{h,c}$ *is a* critical point *of* I_h *if* $I_h'(u_h, v_h; \varphi_h, \psi_h) = 0$ *for all* $\varphi_h \in X_{h,D}$ *and* $\psi_h \in X_{h,c}$, *where*

$$\begin{aligned} I_h'(u_h, v_h; \varphi_h, \psi_h) &= 2a_h(v_h; u_h, \varphi_h) + 2b_h(u_h; v_h, \psi_h), \\ a_h(v_h; u_h, \varphi_h) &:= \int_\Omega \big(P_h(v_h^2) + \eta\big) \nabla u_h \cdot \nabla \varphi_h \, \mathrm{d}x, \\ b_h(u_h; v_h, \psi_h) &:= \int_\Omega \big[P_h(v_h \psi_h) |\nabla u_h|^2 + \alpha P_h\big((v_h - 1)\psi_h\big) + \varepsilon \nabla v_h \cdot \nabla \psi_h\big] \, \mathrm{d}x. \end{aligned}$$

PROPOSITION 2.2. *Let* $(u_h, v_h) \in X_{h,g} \times X_{h,c}$ *be such that* $b_h(u_h; v_h, \psi_h) = 0$ *for all* $\psi_h \in X_{h,c}$; *then* $0 \leq v_h(x) \leq 1$ *for all* $x \in \Omega$.

Proof. Let $(u_h, v_h) \in X_{h,g} \times X_{h,c}$ be such that $b_h(u_h; v_h, \psi_h) = 0$ for all $\psi_h \in X_{h,c}$. Let $v_h = \sum_{j \in N_h} v_j \zeta_j$, and suppose, for contradiction, that there exist subsets J_1 and J_2 of N_h with $v_j > 1$ for all $j \in J_1$ and $v_j < 0$ for all $j \in J_2$. First suppose that J_1 is nonempty and $i \in J_1$ is such that $v_i \geq v_j$ for all $j \in N_h$. Consider the patch of elements $\omega_i := \mathrm{supp}(\zeta_i)$, and define $M_i := \{j \in N_h : x_j \in \omega_i\}$.

On taking $\psi_h = \zeta_i$, we have $b_h(u_h; v_h, \zeta_i) = 0$, which implies that

$$\begin{aligned} \varepsilon \int_{\omega_i} \nabla v_h \cdot \nabla \zeta_i \, \mathrm{d}x &= -\int_{\omega_i} P_h(v_h \zeta_i) |\nabla u_h|^2 \, \mathrm{d}x - \alpha \int_{\omega_i} P_h((v_h - 1)\zeta_i) \, \mathrm{d}x \\ &= -\frac{2v_i}{N!} \sum_{T \subset \omega_i} |\nabla u_h|_T^2 |T| - \frac{2\alpha}{N!}(v_i - 1)|\omega_i| \\ &< 0. \end{aligned} \tag{2.3}$$

Since $v_h = \sum_{j \in N_h} v_j \zeta_j$, on noting that the rows of the stiffness matrix sum to zero, we have

$$\int_{\omega_i} \nabla v_h \cdot \nabla \zeta_i \, \mathrm{d}x = \sum_{j \in M_i} k_{ij} v_j = \sum_{j \in M_i} k_{ij}(v_j - v_i) + \sum_{j \in M_i} k_{ij} v_i = \sum_{j \in M_i} k_{ij}(v_j - v_i).$$

Thus, using the assumption that $k_{ij} \leq 0$ for $i \neq j$, it follows that $\int_{\omega_i} \nabla v_h \cdot \nabla \zeta_i \, \mathrm{d}x \geq 0$, which contradicts (2.3).

A similar argument can be used to contradict the existence of vertices in J_2. ∎

In the finite element approximation, at time $t = t_k$, we seek to find

$$(u_h, v_h) \in \mathrm{argmin}\{I_h(\hat{u}_h, \hat{v}_h) : \hat{u}_h \in X_{h,g},\ \hat{v}_h \in X_{h,c}\}. \tag{2.4}$$

2.2. The alternate minimization algorithm. The minimization of the functional I_h is a nontrivial task, since the term $P_h(v_h^2)\,|\nabla u_h|^2$ renders the functional nonconvex. A number of minimization schemes can be employed; we note, however, that none would in general be able to find the location of global minimizers, at least

Copyright © by SIAM. Unauthorized reproduction of this article is prohibited.

not easily. Instead we must be satisfied with being able to locate *local* minimizers. (In any case, as we have previously noted, it is unclear to us that finding global minimizers of the Francfort–Marigo model is physically justified.)

The minimization will be achieved using an alternate minimization algorithm proposed by Bourdin, Francfort, and Marigo [11]. We state the algorithm for the minimization of I over the infinite-dimensional space $\mathrm{H}^1_g(\Omega) \times \mathrm{H}^1_c(\Omega)$ at time $t = t_k$. The idea is as follows. Although the functional I is nonconvex with respect to the pair (u, v), I is convex with respect to u and v separately. Thus it is a straightforward computation to minimize with respect to one variable at a time. For some termination tolerance `VTOL`, the algorithm proceeds as follows:

1. Set $v^1 = 1$ if $k = 0$ and $v^1 = v(t_{k-1})$ if $k > 0$.
2. For $n = 1, 2, \ldots,$
   - $u^n = \operatorname{argmin}\{I(z, v^n) : z \in \mathrm{H}^1_g(\Omega)\}$;
   - $v^{n+1} = \operatorname{argmin}\{I(u^n, w) : w \in \mathrm{H}^1_c(\Omega)\}$;
   - repeat until $\|v^{n+1} - v^n\|_{L^\infty(\Omega)} < \mathtt{VTOL}$.
3. Set $u(t_k) = u^n$ and $v(t_k) = v^{n+1}$.

The algorithm has been successfully implemented by Bourdin, Francfort, and Marigo [11] and Bourdin [8, 9] for a range of computational examples. However, to date there does not exist a proof of convergence for the algorithm to a minimizer as $n \to \infty$. It appears to us that the proof of [8, Theorem 1] is incomplete, even though the result is certainly correct. The missing arguments can be found in the present paper, in the proofs of Theorems 4.1 and 4.2 (in particular, Step 4 in the proof of Theorem 4.1 and Steps 3 and 4 in the proof of Theorem 4.2).

For a proof of local convergence to isolated local minimizers, see [8, Theorem 2].

Remark 3. The alternate minimization algorithm can be understood as a Newton-type descent method with a special starting guess. To see this, let $u^0 \in \mathrm{H}^1_g(\Omega)$ and $v^1 = \operatorname{argmin}_{\mathrm{H}^1_c(\Omega)} I(u^0, \cdot)$. The first step of the alternate minimization algorithm, computing the pair (u^1, v^2), can be written as

$$\partial_u I(u^1, v^1) = 0 \quad \text{and} \quad \partial_v I(u^1, v^2) = 0, \tag{2.5}$$

where $\partial_u I$ and $\partial_v I$ denote the partial derivatives of I. Since I is quadratic in each of its two coordinates, with nonsingular partial derivatives $\partial_{uu} I$ and $\partial_{vv} I$, the equalities (2.5) are equivalent to

$$\partial_{uu} I(u^0, v^1)(u^1 - u^0) = -\partial_u I(u^0, v^1) \quad \text{and} \quad \partial_{vv} I(u^1, v^1)(v^2 - v^1) = -\partial_v I(u^1, v^1).$$

It can now be easily seen that these two equations are equivalently written as

$$\begin{pmatrix} \partial_{uu} I(u^0, v^1) & 0 \\ 0 & \partial_{vv} I(u^0, v^1) \end{pmatrix} \begin{pmatrix} \bar{u}^{1/2} - u^0 \\ \bar{v}^{1/2} - v^1 \end{pmatrix} = -\begin{pmatrix} \partial_u I(u^0, v^1) \\ \partial_v I(u^0, v^1) \end{pmatrix} \quad \text{and}$$

$$\begin{pmatrix} \partial_{uu} I(\bar{u}^{1/2}, \bar{v}^{1/2}) & 0 \\ 0 & \partial_{vv} I(\bar{u}^{1/2}, \bar{v}^{1/2}) \end{pmatrix} \begin{pmatrix} \bar{u}^1 - \bar{u}^{1/2} \\ \bar{v}^1 - \bar{v}^{1/2} \end{pmatrix} = -\begin{pmatrix} \partial_u I(\bar{u}^{1/2}, \bar{v}^{1/2}) \\ \partial_v I(\bar{u}^{1/2}, \bar{v}^{1/2}) \end{pmatrix},$$

where $(\bar{u}^{1/2}, \bar{v}^{1/2}) := (u^1, v^1)$ and $(\bar{u}^1, \bar{v}^1) := (u^1, v^2)$.

3. Adaptive algorithm. The nature of solutions to the minimization problem strongly motivates the use of an adaptive finite element method for their computation. Such methods use a *local refinement indicator*, based on the computed solution, to identify those elements where mesh refinement would be most beneficial for improving

Copyright © by SIAM. Unauthorized reproduction of this article is prohibited.

the accuracy of the solution. It is now a well-established technique to use residual estimates as refinement indicators [36].

For a critical point (u_h, v_h) of I_h from the finite-dimensional space $X_{h,g} \times X_{h,c}$, we use an estimate of the residual

$$I'(u_h, v_h; \varphi, \psi) \qquad \text{for } \varphi \in \mathrm{H}^1_D(\Omega),\ \psi \in \mathrm{H}^1_c(\Omega) \tag{3.1}$$

in the $\big(\mathrm{H}^1_D(\Omega) \times \mathrm{H}^1_c(\Omega)\big)^*$ norm as a refinement indicator. Note that (3.1) is well defined, since $u_h,\ v_h \in \mathrm{W}^{1,\infty}(\Omega)$. We derive an a posteriori upper bound on this residual in the first part of this section. In the second part, we propose two adaptive finite element algorithms based on this bound to determine mesh refinement.

3.1. Residual estimates. The following interpolation results will be needed for the subsequent residual estimate. Henceforth we use $\lesssim$ to denote $\leq C$, where the positive constant C depends only on the shape-regularity parameter K of the mesh but not on the mesh size.

We remind the reader that, for a node with position x_i, a face e, or an element T, ω_i, ω_e, and ω_T denote the closure of the union of all elements that touch the respective sets (or point). Here, the touching of two sets means that the intersection of their closure is nonempty. Let Δ_i be the maximal set of the form $\overline{B} \cap \overline{\Omega}$ contained within ω_i, where B is a ball with center x_i (cf. [37] for more detail).

For $\chi \in \mathrm{H}^1(\Omega)$, define the *quasi interpolants* $\Pi_{h,D}\,\chi \in X_{h,D}$ and $\Pi_{h,c}\,\chi \in X_{h,c}$ as follows:

$$\big(\Pi_{h,D}\,\chi\big)(x) := \sum_{i \in N_h \setminus N_{h,D}} \left(\frac{1}{|\Delta_i|}\int_{\Delta_i} \chi \,\mathrm{d}x\right) \lambda_i(x), \tag{3.2}$$

$$\big(\Pi_{h,c}\,\chi\big)(x) := \sum_{\substack{i \in N_h \\ x_i \notin \mathrm{CR}_h}} \left(\frac{1}{|\Delta_i|}\int_{\Delta_i} \chi \,\mathrm{d}x\right) \lambda_i(x).$$

This quasi interpolant was defined by Verfürth [37] and was shown to satisfy the following approximation results. Let $\chi \in \mathrm{H}^1_D(\Omega)$, and let $\Pi_{h,D}\,\chi$ be as above; then, for all $T \in \mathcal{T}_h$ and $e \in \mathcal{E}_h$,

$$\|\Pi_{h,D}\,\chi - \chi\|_{\mathrm{H}^s(T)} \lesssim h_T^{1-s} \|\nabla \chi\|_{\mathrm{L}^2(\omega_T)}, \qquad s \in \{0, 1\}, \tag{3.3}$$

$$\|\Pi_{h,D}\,\chi - \chi\|_{\mathrm{L}^2(e)} \lesssim h_e^{1/2} \|\nabla \chi\|_{\mathrm{L}^2(\omega_e)}. \tag{3.4}$$

The same approximation result holds taking $\chi \in \mathrm{H}^1_c(\Omega)$ and replacing $\Pi_{h,D}\,\chi$ with $\Pi_{h,c}\,\chi$.

We also have the following approximation result for the nodal interpolant; see [13, section 4.4]. For all $T \in \mathcal{T}_h$ and $w \in \mathrm{W}^{s,\infty}(T)$,

$$\|w - P_h w\|_{\mathrm{L}^\infty(T)} \lesssim h_T^s |w|_{\mathrm{W}^{s,\infty}(T)}, \qquad s \in \{1, 2\}. \tag{3.5}$$

Before stating the main proposition of this section, it will be useful to introduce the following definition. For $w_h \in X_h$ and all $e \in \mathcal{E}_h$, we define

$$[\![\nabla w_h]\!]_e := \begin{cases} \big|\, \nabla w_h|_{T_1} - \nabla w_h|_{T_2} \,\big| & \text{if } e \subseteq E_h \setminus \partial\Omega, \text{ with } e = \overline{T}_1 \cap \overline{T}_2 \\ & \text{for some } T_1, T_2 \in \mathcal{T}_h, \\ |\nabla w_h \cdot n|_e & \text{if } e \subseteq \partial\Omega\,, \end{cases}$$

where n is the outer unit normal vector to $\partial\Omega$.

Copyright © by SIAM. Unauthorized reproduction of this article is prohibited.

PROPOSITION 3.1. *Let $u_h \in X_{h,g}$, $v_h \in X_{h,c}$ be such that $I_h'(u_h, v_h; \varphi_h, \psi_h) = 0$ for all $\varphi_h \in X_{h,D}$, $\psi_h \in X_{h,c}$; then*

$$|I'(u_h, v_h; \varphi, \psi)| \lesssim \mu_h \|\nabla\varphi\|_{\mathrm{L}^2(\Omega)} + \nu_h \|\nabla\psi\|_{\mathrm{L}^2(\Omega)} \qquad \forall \varphi \in \mathrm{H}^1_D(\Omega),\ \forall \psi \in \mathrm{H}^1_c(\Omega),$$

where μ_h, ν_h are defined as follows:

$$\mu_h := \left[\sum_{T\in\mathcal{T}_h} |\mu_T(u_h, v_h)|^2\right]^{1/2}, \quad \nu_h := \left[\sum_{T\in\mathcal{T}_h} |\nu_T(u_h, v_h)|^2\right]^{1/2}, \tag{3.6}$$

where

$$\begin{aligned}
|\mu_T(u_h, v_h)|^2 &:= h_T^4 \|\nabla v_h\|^4_{\mathrm{L}^\infty(T)} \|\nabla u_h\|^2_{\mathrm{L}^2(T)} + h_T^2 \|2v_h(\nabla v_h \cdot \nabla u_h)\|^2_{\mathrm{L}^2(T)} \\
&\quad + \sum_{e\subseteq\partial T\cap(E_{I,h}\cup E_{N,h})} h_e \|v_h^2 + \eta\|^2_{\mathrm{L}^2(e)} \|[\![\nabla u_h]\!]_e\|^2, \\
|\nu_T(u_h, v_h)|^2 &:= h_T^4 \||\nabla u_h|^2 + \alpha\|^2_{\mathrm{L}^2(T)} \|\nabla v_h\|^2_{\mathrm{L}^\infty(T)} + h_T^2 \|(|\nabla u_h|^2 + \alpha)v_h - \alpha\|^2_{\mathrm{L}^2(T)} \\
&\quad + \varepsilon^2 \sum_{e\subseteq\partial T} h_e \|[\![\nabla v_h]\!]_e\|^2_{\mathrm{L}^2(e)}.
\end{aligned}$$

Proof. Since $I_h'(u_h, v_h; \varphi_h, \psi_h) = 0$ for all $\varphi_h \in X_{h,D}$, $\psi \in X_{h,c}$, it follows that

$$a_h(v_h; u_h, \varphi_h) = 0 \qquad \forall \varphi_h \in X_{h,D} \quad \text{and} \tag{3.7}$$

$$b_h(u_h; v_h, \psi_h) = 0 \qquad \forall \psi_h \in X_{h,c}. \tag{3.8}$$

Let us fix $\varphi \in \mathrm{H}^1_D(\Omega)$ and $\psi \in \mathrm{H}^1_c(\Omega)$; then

$$|I'(u_h, v_h; \varphi, \psi)| \le 2\,|a(v_h; u_h, \varphi)| + 2\,|b(u_h; v_h, \psi)|.$$

Hence we shall examine the two functionals $\varphi \mapsto a(v_h; u_h, \varphi)$ and $\psi \mapsto b(u_h; v_h, \psi)$ separately.

We begin by considering the former. By (3.7), we have

$$\begin{aligned}
|a(v_h; u_h, \varphi)| &\le |a(v_h; u_h, \varphi - \varphi_h)| \\
&\quad + |a(v_h; u_h, \varphi_h) - a_h(v_h; u_h, \varphi_h)| \qquad \forall \varphi_h \in X_{h,D}.
\end{aligned} \tag{3.9}$$

Examining the first term in (3.9),

$$\begin{aligned}
|a(v_h; u_h, \varphi - \varphi_h)| &= \left|\sum_{T\in\mathcal{T}_h} \int_T (v_h^2 + \eta)\nabla u_h \cdot \nabla(\varphi - \varphi_h)\,\mathrm{d}x\right| \\
&= \left|\sum_{T\in\mathcal{T}_h} \left\{\int_T -2v_h(\nabla v_h \cdot \nabla u_h)(\varphi - \varphi_h)\,\mathrm{d}x \right.\right. \\
&\qquad \left.\left. + \int_{\partial T} (v_h^2 + \eta)\nabla u_h \cdot n\,(\varphi - \varphi_h)\,\mathrm{d}s\right\}\right| \\
&\lesssim \sum_{T\in\mathcal{T}_h} \|2v_h(\nabla v_h \cdot \nabla u_h)\|_{\mathrm{L}^2(T)} \|\varphi - \varphi_h\|_{\mathrm{L}^2(T)} \\
&\quad + \sum_{e\subseteq(E_{I,h}\cup E_{N,h})} \int_e [\![\nabla u_h]\!]_e |v_h^2 + \eta||\varphi - \varphi_h|\,\mathrm{d}s \\
&\le \sum_{T\in\mathcal{T}_h} \|2v_h(\nabla v_h \cdot \nabla u_h)\|_{\mathrm{L}^2(T)} \|\varphi - \varphi_h\|_{\mathrm{L}^2(T)} \\
&\quad + \sum_{e\subseteq(E_{I,h}\cup E_{N,h})} [\![\nabla u_h]\!]_e \|v_h^2 + \eta\|_{\mathrm{L}^2(e)} \|\varphi - \varphi_h\|_{\mathrm{L}^2(e)}.
\end{aligned}$$

Copyright © by SIAM. Unauthorized reproduction of this article is prohibited.

Since this inequality is true for all $\varphi_h \in X_{h,D}$, we choose $\varphi_h = \Pi_{h,D}\,\varphi$ and use the approximation results (3.3) and (3.4) to obtain

$$\begin{aligned}
|a(v_h;u_h,\varphi-\varphi_h)| &\lesssim \sum_{T\in\mathcal{T}_h} h_T\,\|2v_h(\nabla v_h\cdot\nabla u_h)\|_{\mathrm{L}^2(T)}\|\nabla\varphi\|_{\mathrm{L}^2(\omega_T)}\\
&\quad+\sum_{e\subseteq(E_{I,h}\cup E_{N,h})} h_e^{1/2}\|v_h^2+\eta\|_{\mathrm{L}^2(e)}[\![\nabla u_h]\!]_e\|\nabla\varphi\|_{\mathrm{L}^2(\omega_e)}\\
&\lesssim \left[\sum_{T\in\mathcal{T}_h} h_T^2\|2v_h(\nabla v_h\cdot\nabla u_h)\|^2_{\mathrm{L}^2(T)}\right]^{1/2}\|\nabla\varphi\|_{\mathrm{L}^2(\Omega)}\\
&\quad+\left[\sum_{e\subseteq(E_{I,h}\cup E_{N,h})} h_e\|v_h^2+\eta\|^2_{\mathrm{L}^2(e)}[\![\nabla u_h]\!]_e^2\right]^{1/2}\|\nabla\varphi\|_{\mathrm{L}^2(\Omega)}\\
&\lesssim \left[\sum_{T\in\mathcal{T}_h}\left\{ h_T^2\|2v_h(\nabla v_h\cdot\nabla u_h)\|^2_{\mathrm{L}^2(T)}\right.\right.\\
&\quad\left.\left.+\sum_{e\subseteq\partial T\cap(E_{I,h}\cup E_{N,h})} h_e\|v_h^2+\eta\|^2_{\mathrm{L}^2(e)}\,[\![\nabla u_h]\!]_e^2\right\}\right]^{1/2}\|\nabla\varphi\|_{\mathrm{L}^2(\Omega)}.
\end{aligned}$$

Using the approximation result (3.5) for the nodal interpolant and (3.3) with $s=1$, we can bound the second term in (3.9) as follows:

$$\begin{aligned}
&|a(v_h;u_h,\varphi_h)-a_h(v_h;u_h,\varphi_h)|\\
&\quad=\left|\int_\Omega\{v_h^2-P_h(v_h^2)\}\nabla u_h\cdot\nabla\varphi_h\,\mathrm{d}x\right|\\
&\quad\le\sum_{T\in\mathcal{T}_h}\int_T|v_h^2-P_h(v_h^2)|\,|\nabla u_h|\,|\nabla\varphi_h|\,\mathrm{d}x\\
&\quad\le\sum_{T\in\mathcal{T}_h}\|v_h^2-P_h(v_h^2)\|_{\mathrm{L}^\infty(T)}\|\nabla u_h\|_{L^2(T)}\|\nabla\varphi_h\|_{\mathrm{L}^2(T)}\\
&\quad\lesssim\sum_{T\in\mathcal{T}_h} h_T^2\,\|\nabla v_h\|^2_{\mathrm{L}^\infty(T)}\|\nabla u_h\|_{\mathrm{L}^2(T)}\,\|\nabla\varphi\|_{\mathrm{L}^2(\omega_T)}\\
&\quad\lesssim\left[\sum_{T\in\mathcal{T}_h} h_T^4\|\nabla v_h\|^4_{\mathrm{L}^\infty(T)}\|\nabla u_h\|^2_{\mathrm{L}^2(T)}\right]^{1/2}\|\nabla\varphi\|_{\mathrm{L}^2(\Omega)}.
\end{aligned}\tag{3.10}$$

Therefore,

$$|a(v_h;u_h,\varphi)|\lesssim\left[\sum_{T\in\mathcal{T}_h}|\mu_T(u_h,v_h)|^2\right]^{1/2}\|\nabla\varphi\|_{\mathrm{L}^2(\Omega)},$$

Copyright © by SIAM. Unauthorized reproduction of this article is prohibited.

where

$$|\mu_T(u_h,v_h)|^2 = h_T^4\|\nabla v_h\|^4_{\mathrm{L}^\infty(T)}\|\nabla u_h\|^2_{\mathrm{L}^2(T)} + h_T^2\|2v_h(\nabla v_h\cdot\nabla u_h)\|^2_{\mathrm{L}^2(T)} + \sum_{e\subseteq\partial T\cap(E_{I,h}\cup E_{N,h})} h_e\|v_h^2+\eta\|^2_{\mathrm{L}^2(e)}\,[\![\nabla u_h]\!]_e^2.$$

Now let us consider $\psi\mapsto b(u_h;v_h,\psi)$. For all $\psi_h\in X_{h,c}$, it follows from (3.8) that

$$|b(u_h;v_h,\psi)| \le |b(u_h;v_h,\psi-\psi_h)| + |b(u_h;v_h,\psi_h)-b_h(u_h;v_h,\psi_h)|. \tag{3.11}$$

Considering the first term in (3.11),

$$\begin{aligned}
&|b(u_h;v_h,\psi-\psi_h)|\\
&\quad= \left|\sum_{T\in\mathcal{T}_h}\int_T \left[\{\,(|\nabla u_h|^2+\alpha)v_h-\alpha\}(\psi-\psi_h)\;+\;\varepsilon\nabla v_h\;\cdot\nabla(\psi-\psi_h)\right]\mathrm{d}x\right|\\
&\quad\le \sum_{T\in\mathcal{T}_h}\|(|\nabla u_h|^2+\alpha)v_h-\alpha\|_{\mathrm{L}^2(T)}\|\psi-\psi_h\|_{\mathrm{L}^2(T)}\\
&\qquad+\varepsilon\left|\sum_{T\in\mathcal{T}_h}\int_{\partial T}(\psi-\psi_h)\,\nabla v_h\;\cdot\;n\,\mathrm{d}s\right|\\
&\quad\lesssim \sum_{T\in\mathcal{T}_h}\|\,(\,|\nabla u_h|^2\;+\;\alpha)v_h-\alpha\|_{\mathrm{L}^2(T)}\|\psi-\psi_h\|_{\mathrm{L}^2(T)}\\
&\qquad+\varepsilon\sum_{e\subseteq E_h}\|\psi-\psi_h\|_{\mathrm{L}^2(e)}\|[\![\nabla v_h]\!]_e\|_{\mathrm{L}^2(e)}.
\end{aligned}$$

This is true for all $\psi_h\in X_{h,c}$, so taking $\psi_h=\Pi_{h,c}\,\psi$ it follows that

$$\begin{aligned}
|b(u_h;v_h,\psi-\psi_h)| &\lesssim \sum_{T\in\mathcal{T}_h} h_T\|\,(\,|\nabla u_h|^2\;+\;\alpha)v_h-\alpha\|_{\mathrm{L}^2(T)}\|\nabla\psi\|_{\mathrm{L}^2(\omega_T)}\\
&\quad+\varepsilon\sum_{e\subseteq E_h} h_e^{1/2}\|[\![\nabla v_h]\!]_e\|_{\mathrm{L}^2(e)}\|\nabla\psi\|_{\mathrm{L}^2(\omega_e)}\\
&\lesssim \left[\sum_{T\in\mathcal{T}_h} h_T^2\|(\,|\nabla u_h|^2\;+\;\alpha)v_h-\alpha\|^2_{\mathrm{L}^2(T)}\right]^{1/2}\|\nabla\psi\|_{\mathrm{L}^2(\Omega)}\\
&\quad+\varepsilon\left[\sum_{e\subseteq E_h} h_e\|[\![\nabla v_h]\!]_e\|^2_{\mathrm{L}^2(e)}\right]^{1/2}\|\nabla\psi\|_{\mathrm{L}^2(\Omega)}\\
&\lesssim \left[\sum_{T\in\mathcal{T}_h}\left\{\,h_T^2\|\,(|\nabla u_h|^2\;+\;\alpha)v_h-\alpha\|^2_{\mathrm{L}^2(T)}\right.\right.\\
&\qquad\left.\left.+\;\varepsilon^2\sum_{e\subseteq\partial T} h_e\|[\![\nabla v_h]\!]_e\|^2_{\mathrm{L}^2(e)}\right\}\right]^{1/2}\|\nabla\psi\|_{\mathrm{L}^2(\Omega)}.
\end{aligned}$$

Finally we bound the second term in (3.11), noting that we have now fixed $\psi_h=$

Copyright © by SIAM. Unauthorized reproduction of this article is prohibited.

$\Pi_{h,c}\,\psi$:

$$
\begin{aligned}
(3.12)\qquad & |b(u_h;v_h,\psi_h)-b_h(u_h;v_h,\psi_h)| \\
&= \left|\int_\Omega (v_h\psi_h - P_h(v_h\psi_h))(|\nabla u_h|^2+\alpha)\,\mathrm{d}x\right| \\
&\le \sum_{T\in\mathcal{T}_h}\int_T |v_h\psi_h - P_h(v_h\psi_h)|\,(|\nabla u_h|^2+\alpha)\,\mathrm{d}x \\
&\lesssim \sum_{T\in\mathcal{T}_h} h_T^{N/2}\|\,|\nabla u_h|^2+\alpha\|_{\mathrm{L}^2(T)}\|v_h\psi_h - P_h(v_h\psi_h)\|_{\mathrm{L}^\infty(T)} \\
&\lesssim \sum_{T\in\mathcal{T}_h} h_T^{(N/2)+2}\|\,|\nabla u_h|^2+\alpha\|_{\mathrm{L}^2(T)}\,|v_h\psi_h|_{\mathrm{W}^{2,\infty}(T)} \\
&\lesssim \sum_{T\in\mathcal{T}_h} h_T^{(N/2)+2}\|\,|\nabla u_h|^2+\alpha\|_{\mathrm{L}^2(T)}\,\|\nabla v_h\|_{\mathrm{L}^\infty(T)}\|\nabla\psi_h\|_{\mathrm{L}^\infty(T)}.
\end{aligned}
$$

Using the equivalence of norms on a finite-dimensional space and the shape regularity of $\mathcal{T}_h$, we have

$$
\begin{aligned}
&|b(u_h;v_h,\psi_h)-b_h(u_h;v_h,\psi_h)| \\
&\quad\lesssim \sum_{T\in\mathcal{T}_h} h_T^{(N/2)+2-(N/2)}\|\,|\nabla u_h|^2+\alpha\|_{\mathrm{L}^2(T)}\|\nabla v_h\|_{\mathrm{L}^\infty(T)}\,\|\nabla\psi_h\|_{\mathrm{L}^2(T)} \\
&\quad\le \left[\sum_{T\in\mathcal{T}_h} h_T^4\||\nabla u_h|^2+\alpha\|^2_{\mathrm{L}^2(T)}\|\nabla v_h\|^2_{\mathrm{L}^\infty(T)}\right]^{1/2}\|\nabla\psi\|_{\mathrm{L}^2(\Omega)}.
\end{aligned}
$$

Therefore,

$$
|b(u_h;v_h,\psi)| \lesssim \left[\sum_{T\in\mathcal{T}_h}|\nu_T(u_h,v_h)|^2\right]^{1/2}\|\nabla\psi\|_{\mathrm{L}^2(\Omega)},
$$

where

$$
\begin{aligned}
|\nu_T(u_h,v_h)|^2 = h_T^4\||\nabla u_h|^2+\alpha\|^2_{\mathrm{L}^2(T)}\|\nabla v_h\|^2_{\mathrm{L}^\infty(T)} + h_T^2\|(|\nabla u_h|^2+\alpha)v_h-\alpha\|^2_{\mathrm{L}^2(T)} \\
+\varepsilon^2\sum_{e\subseteq\partial T} h_e\,\|[\![\nabla v_h]\!]_e\|^2_{\mathrm{L}^2(e)}. \qquad \square
\end{aligned}
$$

We use $\mu_T(u_h,v_h)$ as a local refinement indicator for u_h, use $\nu_T(u_h,v_h)$ as a local refinement indicator for v_h, and define

$$
(3.13)\qquad E_T(u_h,v_h) := \left[\big|\mu_T(u_h,v_h)\big|^2+\big|\nu_T(u_h,v_h)\big|^2\right]^{1/2}\qquad \forall T\in\mathcal{T}_h.
$$

Remark 4. We are in fact estimating the $\big(\mathrm{H}^1_D(\Omega)\times\mathrm{H}^1_c(\Omega)\big)^*$ norm of the gradient of I, since

$$
\begin{aligned}
\|I'(u_h,v_h)\|_{(\mathrm{H}^1_D(\Omega)\times\mathrm{H}^1_c(\Omega))^*} &= \sup_{\substack{\varphi\in\mathrm{H}^1_D(\Omega),\\ \psi\in\mathrm{H}^1_c(\Omega)}}\frac{|I'(u_h,v_h;\varphi,\psi)|}{\left[\|\varphi\|^2_{\mathrm{H}^1(\Omega)}+\|\psi\|^2_{\mathrm{H}^1(\Omega)}\right]^{1/2}} \\
&\lesssim \left[\sum_{T\in\mathcal{T}_h}|E_T(u_h,v_h)|^2\right]^{1/2}.
\end{aligned}
$$

Copyright © by SIAM. Unauthorized reproduction of this article is prohibited.

3.2. Adaptive algorithm. We now propose two adaptive algorithms for computing local minimizers of I. The difference between the two algorithms is the stage at which the adaptive refinement of the mesh takes place. In Algorithm 1, this occurs after the alternate minimization algorithm has converged, whilst in Algorithm 2 the mesh is refined at each step of the alternate minimization algorithm.

There are two user-specified tolerances associated with the algorithms: `VTOL` is the tolerance which determines when to halt the alternate minimization loop, whilst `REFTOL` is the tolerance determining when to halt the refinement loop. The *marking parameter* θ is a fixed number lying in the interval $(0, 1]$.

In Algorithm 1, we denote the mesh at the jth level of refinement by $\mathcal{T}_j$ with $h_j := \max_{T\in\mathcal{T}_j} \operatorname{diam}(T)$ for $j \in \mathbb{N}$. In Algorithm 2, the mesh is also dependent on the alternate minimization step; accordingly, within each alternate minimization step $n \in \{m/2 : m \in \mathbb{N}\}$, we denote the mesh at the jth level of refinement by $\mathcal{T}_j^n$ with $h_j^n := \max_{T\in\mathcal{T}_j^n} \operatorname{diam}(T)$ for $j \in \mathbb{N}$.

Algorithm 1.

1. Input: Initial crack field v_0 and initial mesh $\mathcal{T}_1$.
2. For $j = 1, 2, \ldots,$
   (a) set $v_j^1 = v_{j-1}$;
   (b) for $n = 1, 2, \ldots,$
   - $u_j^n :=$ argmin $\{I_{h_j}(z, v_j^n) : z \in X_{h_j,g}\}$;
   - $v_j^{n+1} :=$ argmin $\{I_{h_j}(u_j^n, z) : z \in X_{h_j,c}\}$;
   - repeat until $\|v_j^{n+1} - v_j^n\|_{\mathrm{L}^\infty(\Omega)} <$ `VTOL`;

   (c) set $v_j = v_j^{n+1}$, $u_j = u_j^n$;
   (d) if $\big[\sum_{T\in\mathcal{T}_j} |E_T(u_j, v_j)|^2\big]^{1/2} >$ `REFTOL`,
   - find the smallest set $M_j \subseteq \mathcal{T}_j$ such that $\sum_{T\in M_j} |E_T(u_j, v_j)|^2 \geq \theta \sum_{T\in\mathcal{T}_j} |E_T(u_j, v_j)|^2$;
   - refine elements in M_j to obtain the new mesh $\mathcal{T}_{j+1}$;

   (e) repeat until $\big[\sum_{T\in\mathcal{T}_j} |\, E_T(u_j, v_j)\,|^2\,\big]^{1/2} \leq$ `REFTOL`.
3. Set $u_h(t_k) = u_j$ and $v_h(t_k) = v_j$.

Algorithm 2.

1. Input: Initial crack field v^1 and initial mesh $\mathcal{T}^{1/2}$.
2. For $n = 1, 2, \ldots,$
   (a) set $\mathcal{T}_1^n = \mathcal{T}^{n-1/2}$;
   (b) for $j = 1, 2, \ldots,$
   - compute $u_j^n :=$ argmin $\{I_{h_j^n}(z, v^n) : z \in X_{h_j^n,g}\}$;
   - if $\big[\sum_{T\in\mathcal{T}_j^n} |\,\mu_T(u_j^n, v^n)\,|^2\,\big]^{1/2} >$ `REFTOL`$/\sqrt{2}$,
     - find the smallest set $M_j \subseteq \mathcal{T}_j^n$ such that $\sum_{T\in M_j} |\mu_T(u_j^n, v_j)|^2 \geq \theta \sum_{T\in\mathcal{T}_j^n} |\mu_T(u_j^n, v_j)|^2$;
     - refine elements in M_j to obtain the new mesh $\mathcal{T}_{j+1}^n$;
   - repeat until $\big[\sum_{T\in\mathcal{T}_j^n} |\,\mu_T(u_j^n, v^n)\,|^2\,\big]^{1/2} \leq$ `REFTOL`$/\sqrt{2}$;

Copyright © by SIAM. Unauthorized reproduction of this article is prohibited.

(c) set $u^n = u_j^n$, $\mathcal{T}^n = \mathcal{T}_j^n$, and $\mathcal{T}_1^{n+1/2} = \mathcal{T}^n$;

(d) for $j = 1, 2, \ldots,$

- compute $v_j^{n+1} := \operatorname{argmin} \{I_{h_j^{n+1/2}}(u^n, z) : z \in X_{h_j^{n+1/2},c}\}$;
- if $\big[\sum_{T\in\mathcal{T}_j^{n+1/2}} |\,\nu_T(u^n, v_j^{n+1})\,|^2\,\big]^{1/2} > \texttt{REFTOL}/\sqrt{2}$,
  - find the smallest set $M_j \subseteq \mathcal{T}_j^{n+1/2}$ such that $\sum_{T\in M_j} |\nu_T(u^n, v_j^{n+1})|^2 \geq \theta \sum_{T\in\mathcal{T}_j^{n+1/2}} |\nu_T(u^n, v_j^{n+1})|^2$;
  - refine elements in M_j to obtain the new mesh $\mathcal{T}_{j+1}^{n+1/2}$;
- repeat until $\big[\sum_{T\in\mathcal{T}_j^{n+1/2}} |\,\nu_T(u^n, v_j^{n+1})\,|^2\,\big]^{1/2} \leq \texttt{REFTOL}/\sqrt{2}$;

(e) set $v^{n+1} = v_j^{n+1}$ and $\mathcal{T}^{n+1/2} = \mathcal{T}_j^{n+1/2}$;

(f) repeat until $\|v^{n+1} - v^n\|_{\mathrm{L}^\infty(\Omega)} < \texttt{VTOL}$.

3. Set $v_h(t_k) = v^{n+1}$ and $u_h(t_k) = u^n$.

The marking strategy used to identify elements for refinement is due to Dörfler [21]. In our implementation, the refinement of the mesh is achieved using the newest node bisection method [29], which guarantees a uniform bound on the shape-regularity parameters of the generated family of meshes.

Remark 5. We return to address a possible criticism, briefly mentioned at the end of section 1.2, that a locally refined mesh may favor certain crack paths over others. For example, for Algorithm 1, it is conceivable that an ill-chosen initial mesh may have this effect.

Algorithm 2, however, is designed so as to ensure that local adaptive refinement does not influence the formation of cracks beyond the usual numerical perturbation. Namely, at each alternate minimization step, the error between the numerical and the exact solutions is controlled by the refinement tolerance, in the spirit of standard adaptive finite element algorithms for linear elliptic problems. Therefore, steps (b) and (d) compute the exact solution up to a specified tolerance. For example, if the *exact* solution for one alternate minimization step initiates a new crack in a region of the domain where the mesh is coarse, then the adaptive mesh refinement algorithm of step (b) or (d) will force mesh refinement in that region, provided the refinement tolerance is set sufficiently small. In fact, local mesh refinement allows us to compute with a smaller regularization parameter ϵ than one could conceivably use on a uniform mesh whose mesh size is equal to the minimum mesh size in an adaptively refined mesh, and this, in turn, results in a more reliable computation of crack paths.

Finally, we present a modification of Algorithm 2, which is useful for theoretical purposes.

ALGORITHM 2′. In step n of Algorithm 2′, we replace REFTOL by $\texttt{REFTOL}_n$, and we require that $\texttt{REFTOL}_n \to 0$ as $n \to \infty$. Furthermore, we remove the termination condition (f).

Remark 6. In order for Algorithms 2 and 2′ to be meaningful, steps (b) and (d) in Algorithm 2 need to terminate after a finite number of iterations. Without the mass lumping approximation, this would follow immediately from standard convergence results for adaptive finite element methods for linear elliptic problems [15]. It is beyond the scope of this paper to prove that the same results remain true in the presence of mass lumping; however, we do not expect serious difficulties in extending existing results.

Instead, in Theorem 4.2 we shall make the following assumption:

(A) Steps (b) and (d) in Algorithm 2 terminate in a finite number of iterations.

Copyright © by SIAM. Unauthorized reproduction of this article is prohibited.

We now state some properties of the sequences generated by the preceding algorithms, which will prove useful later in the convergence analysis.

LEMMA 3.2. *The sequence* $((u_j, v_j))_{j=1}^{\infty} \subseteq X_{h_j,g} \times X_{h_j,c}$ *generated by Algorithm* 1 *satisfies the following properties:*

1. $0 \le v_j(x) \le 1$ *on* Ω *for all* $j \in \mathbb{N}$*;*
2. $((u_j, v_j))_{j=1}^{\infty}$ *is bounded in* $\mathrm{H}^1(\Omega) \times \mathrm{H}^1(\Omega)$.

Proof. The first property follows from Proposition 2.2. In order to prove the second property, note that $u_j := u_j^n$, $v_j := v_j^{n+1}$, where

$$a_{h_j}(v_j^n; u_j^n, \varphi_j) = 0 \qquad \forall \varphi_j \in X_{h_j,D}, \tag{3.14}$$

$$b_{h_j}(u_j^n; v_j^{n+1}, \psi_j) = 0 \qquad \forall \psi_j \in X_{h_j,c}. \tag{3.15}$$

Taking $\varphi_j = u_j^n - P_{h_j} g \in X_{h_j,D}$ in (3.14), we have

$$\int_\Omega (P_{h_j}((v_j^n)^2) + \eta) \nabla u_j^n \cdot \nabla (u_j^n - P_{h_j} g) \, \mathrm{d}x = 0.$$

Hence,

$$\begin{aligned} \eta \|\nabla u_j^n\|_{\mathrm{L}^2(\Omega)}^2 &\le \int_\Omega (P_{h_j}((v_j^n)^2) + \eta) \nabla u_j^n \cdot \nabla P_{h_j} g \, \mathrm{d}x \\ &\le (1+\eta) \|\nabla u_j^n\|_{\mathrm{L}^2(\Omega)} \|\nabla P_{h_j} g\|_{\mathrm{L}^2(\Omega)}, \end{aligned}$$

and since we have assumed that $g \in X_{h_j,g}$,

$$\|\nabla u_j^n\|_{\mathrm{L}^2(\Omega)} \le \frac{1+\eta}{\eta} \|\nabla g\|_{\mathrm{L}^2(\Omega)}.$$

Therefore, $(\|\nabla u_j\|_{\mathrm{L}^2(\Omega)})_{j=1}^{\infty}$ is a bounded sequence, which by a variant of the Friedrichs inequality implies that $(\|u_j\|_{\mathrm{L}^2(\Omega)})_{j=1}^{\infty}$ is bounded as well; to see this, note that $u_j - P_{h_j} g \in \mathrm{H}_D^1(\Omega)$, and so, since $P_{h_j} g = g$,

$$\begin{aligned} \|u_j\|_{\mathrm{L}^2(\Omega)} &\le \|u_j - g\|_{\mathrm{L}^2(\Omega)} + \|g\|_{\mathrm{L}^2(\Omega)} \le c_* \|\nabla (u_j - g)\|_{\mathrm{L}^2(\Omega)} + \|g\|_{\mathrm{L}^2(\Omega)} \\ &\le c_* \|\nabla u_j\|_{\mathrm{L}^2(\Omega)} + (c_*^2 + 1)^{1/2} \|g\|_{\mathrm{H}^1(\Omega)}, \end{aligned}$$

where $c_* = c_*(\Omega) > 0$ is the constant in the Friedrichs inequality. This implies that $(u_j)_{j=1}^{\infty}$ is bounded in $\mathrm{H}^1(\Omega)$.

Taking $\psi_j = v_j^{n+1} \in X_{h_j,c}$ in (3.15), we have

$$\int_\Omega P_{h_j}((v_j^{n+1})^2) |\nabla u_j^n|^2 \, \mathrm{d}x + \alpha \int_\Omega v_j^{n+1}(v_j^{n+1} - 1) \, \mathrm{d}x + \varepsilon \int_\Omega |\nabla v_j^{n+1}|^2 \, \mathrm{d}x = 0,$$

which implies that

$$\varepsilon \|\nabla v_j^{n+1}\|_{\mathrm{L}^2(\Omega)}^2 \le \alpha \int_\Omega (1 - v_j^{n+1}) v_j^{n+1} \, \mathrm{d}x \le \frac{\alpha |\Omega|}{4}.$$

Hence $(\|\nabla v_j\|)_{j=1}^{\infty}$ is bounded in $\mathrm{L}^2(\Omega)$, and since $(v_j)_{j=1}^{\infty}$ is bounded in $\mathrm{L}^\infty(\Omega)$, it is also bounded in $\mathrm{L}^2(\Omega)$. Thus $((u_j, v_j))_{j=1}^{\infty}$ is bounded in $\mathrm{H}^1(\Omega) \times \mathrm{H}^1(\Omega)$. ∎

LEMMA 3.3. *The sequence* $((u^n, v^n))_{n=1}^{\infty} \subseteq X_{h^n,g} \times X_{h^n,c}$ *generated by Algorithm* $2'$ *satisfies the following properties:*

1. $0 \le v^n(x) \le 1$ *on* Ω *for all* $n \in \mathbb{N}$*;*

Copyright © by SIAM. Unauthorized reproduction of this article is prohibited.

2. $((u^n, v^n))_{n=1}^{\infty}$ *is a bounded sequence in* $\mathrm{H}^1(\Omega) \times \mathrm{H}^1(\Omega)$*;*
3. $I_{h^n}(u^n, v^n) \leq I_{h^{n-1/2}}(u^{n-1}, v^n) \leq I_{h^{n-1}}(u^{n-1}, v^{n-1})$ *for all* $n \in \mathbb{N}$*,* $n \geq 2$*;*
4. $\lim_{n\to\infty} |I(u^n, v^{n+1}) - I_{h^{n+1/2}}(u^n, v^{n+1})| = 0$*;*
5. $\lim_{n\to\infty} |I(u^n, v^n) - I_{h^n}(u^n, v^n)| = 0$*;*
6. $\liminf_{n\to\infty} I(u^n, v^n) \leq \liminf_{n\to\infty} I(u^{n-1}, v^n) \leq \liminf_{n\to\infty} I(u^{n-1}, v^{n-1})$.

Proof. Properties 1 and 2 follow in a manner similar to that of Lemma 3.2.

To show property 3, recall that $u^n = \operatorname{argmin}\{I_{h^n}(z, v^n) : z \in X_{h^n,g}\}$; therefore

$$I_{h^n}(u^n, v^n) \leq I_{h^n}(u^{n-1}, v^n).$$

Note that on each element $T \in \mathcal{T}_{h^{n-1/2}}$ the function $(v^n)^2$ is convex. Note also that on each element $T \in \mathcal{T}_{h^{n-1/2}}$ the function $P_{h^{n-1/2}}((v^n)^2)$ is linear and interpolates $(v^n)^2$, whilst $P_{h^n}((v^n)^2)$ is a piecewise linear function that interpolates $(v^n)^2$ at a greater or equal number of points than $P_{h^{n-1/2}}((v^n)^2)$ does. It therefore follows that

$$(v^n)^2 \leq P_{h^n}((v^n)^2) \leq P_{h^{n-1/2}}((v^n)^2). \tag{3.16}$$

Hence,

$$I_{h^n}(u^{n-1}, v^n) \leq I_{h^{n-1/2}}(u^{n-1}, v^n),$$

which proves the left-hand inequality. The right-hand inequality can be shown similarly.

In order to show property 4, note that

$$\begin{aligned} |I(u^n, v^{n+1}) - I_{h^{n+1/2}}(u^n, v^{n+1})| &= \left| \int_\Omega \left[(v^{n+1})^2 - P_{h^{n+1/2}}((v^{n+1})^2)\right](|\nabla u^n|^2 + \alpha)\,\mathrm{d}x \right| \\ &= |b(u^n; v^{n+1}, v^{n+1}) - b_{h^{n+1/2}}(u^n; v^{n+1}, v^{n+1})|, \end{aligned}$$

which is one of the terms bounded in the residual estimate $\psi \mapsto b(u^n; v^{n+1}, \psi)$, with $\psi = v^{n+1}$ (see (3.11)). Therefore,

$$|I(u^n, v^{n+1}) - I_{h^{n+1/2}}(u^n, v^{n+1})| \lesssim \nu_{h^{n+1/2}}(u^n, v^{n+1}) \|\nabla v^{n+1}\|_{\mathrm{L}^2(\Omega)}.$$

Since $\lim_{n\to\infty} \texttt{REFTOL}_n = 0$, it follows that $\lim_{n\to\infty} \nu_{h^{n+1/2}}(u^n, v^{n+1}) = 0$; therefore

$$\lim_{n\to\infty} |I(u^n, v^{n+1}) - I_{h^{n+1/2}}(u^n, v^{n+1})| = 0.$$

The proof of property 5 uses the same ideas but is slightly more involved. We have

$$\begin{aligned} |I(u^n, v^n) - I_{h^n}(u^n, v^n)| &= \left| \int_\Omega \left[(v^n)^2 - P_{h^n}((v^n)^2)\right](|\nabla u^n|^2 + \alpha)\,\mathrm{d}x \right| \\ &\leq \left| \int_\Omega \left[(v^n)^2 - P_{h^n}((v^n)^2)\right] \nabla u^n \cdot \nabla(u^n - u^{n-1})\,\mathrm{d}x \right| \\ &\quad + \left| \int_\Omega \left[(v^n)^2 - P_{h^n}((v^n)^2)\right](\nabla u^n \cdot \nabla u^{n-1} + \alpha)\,\mathrm{d}x \right| \\ &= |a(v^n; u^n, u^n - u^{n-1}) - a_{h^n}(v^n; u^n, u^n - u^{n-1})| \\ &\quad + \left| \int_\Omega \left[(v^n)^2 - P_{h^n}((v^n)^2)\right](\nabla u^n \cdot \nabla u^{n-1} + \alpha)\,\mathrm{d}x \right|. \end{aligned}$$

Copyright © by SIAM. Unauthorized reproduction of this article is prohibited.

Note that

$$\begin{aligned}
&\left|\int_\Omega \left[(v^n)^2 - P_{h^n}((v^n)^2)\right](\nabla u^n \cdot \nabla u^{n-1} + \alpha)\,\mathrm{d}x\right| \\
&\quad\le \frac{1}{2}\int_\Omega \left|(v^n)^2 - P_{h^n}((v^n)^2)\right|(|\nabla u^n|^2 + \alpha)\,\mathrm{d}x \\
&\qquad + \frac{1}{2}\int_\Omega \left|(v^n)^2 - P_{h^n}((v^n)^2)\right|(|\nabla u^{n-1}|^2 + \alpha)\,\mathrm{d}x \\
&\quad\le \frac{1}{2}\int_\Omega \left|(v^n)^2 - P_{h^n}((v^n)^2)\right|(|\nabla u^n|^2 + \alpha)\,\mathrm{d}x \\
&\qquad + \frac{1}{2}\int_\Omega \left|(v^n)^2 - P_{h^{n-1/2}}((v^n)^2)\right|(|\nabla u^{n-1}|^2 + \alpha)\,\mathrm{d}x \\
&\quad= \frac{1}{2}|I(u^n, v^n) - I_{h^n}(u^n, v^n)| + \frac{1}{2}|b(u^{n-1}; v^n, v^n) - b_{h^{n-1/2}}(u^{n-1}; v^n, v^n)|,
\end{aligned}$$

where we have used (3.16) in the third line.

Therefore,

$$\begin{aligned}
|I(u^n, v^n) - I_{h^n}(u^n, v^n)| \le{}& 2|a(v^n; u^n, u^n - u^{n-1}) - a_{h^n}(v^n; u^n, u^n - u^{n-1})| \\
&+ |b(u^{n-1}; v^n, v^n) - b_{h^{n-1/2}}(u^{n-1}; v^n, v^n)|.
\end{aligned}$$

Noting that the terms on the right-hand side appear in the bounds for the residual estimates $\varphi \mapsto a(v^n; u^n, \varphi)$, with $\varphi = u^n - u^{n-1}$ (see (3.9)) and $\psi \mapsto b(u^{n-1}; v^n, \psi)$, with $\psi = v^n$ (see (3.11)) we have

$$\begin{aligned}
&|I(u^n, v^n) - I_{h^n}(u^n, v^n)| \\
&\quad\lesssim 2\mu_{h^n}(u^n, v^n)\|\nabla(u^n - u^{n-1})\|_{\mathrm{L}^2(\Omega)} + \nu_{h^{n-1/2}}(u^{n-1}, v^n)\|\nabla v^n\|_{\mathrm{L}^2(\Omega)}.
\end{aligned}$$

Since $\lim_{n\to\infty} \texttt{REFTOL}_n = 0$, it follows that $\lim_{n\to\infty} \mu_{h^n}(u^n, v^n) = 0$ and $\lim_{n\to\infty} \nu_{h^{n-1/2}}(u^{n-1}, v^n) = 0$; therefore

$$\lim_{n\to\infty} |I(u^n, v^n) - I_{h^n}(u^n, v^n)| = 0.$$

Finally, we show property 6; we have

$$\begin{aligned}
&I(u^n, v^n) \\
&\quad\le I_{h^n}(u^n, v^n) + |I(u^n, v^n) - I_{h^n}(u^n, v^n)| \\
&\quad\le I_{h^{n-1/2}}(u^{n-1}, v^n) + |I(u^n, v^n) - I_{h^n}(u^n, v^n)| \\
&\quad\le I(u^{n-1}, v^n) + |I(u^{n-1}, v^n) - I_{h^{n-1/2}}(u^{n-1}, v^n)| + |I(u^n, v^n) - I_{h^n}(u^n, v^n)|,
\end{aligned}$$

where we have used property 3 in the second line. On letting $n \to \infty$ and using properties 4 and 5,

$$\liminf_{n\to\infty} I(u^n, v^n) \le \liminf_{n\to\infty} I(u^{n-1}, v^n).$$

The right-hand inequality follows in a similar manner. ∎

Copyright © by SIAM. Unauthorized reproduction of this article is prohibited.

4. Convergence analysis. In this section, we state and prove two results that support the use of the adaptive algorithms proposed in the previous section.

Provided that Algorithm 1 terminates for any given input (we are in fact unable to prove this at present), then Theorem 4.1 demonstrates convergence of the numerical solutions for decreasing tolerance `REFTOL` to a critical point of I.

THEOREM 4.1. *Assume that Ω is an open bounded domain in $\mathbb{R}^N$. Suppose that there exists a sequence $((u_j, v_j))_{j=1}^{\infty} \subset \mathrm{H}^1_g(\Omega) \times \mathrm{H}^1_c(\Omega)$, $0 \le v_j(x) \le 1$ a.e. in Ω such that*

$$a(v_j; u_j, \varphi) \le \mu_j \|\nabla \varphi\|_{\mathrm{L}^2(\Omega)} \qquad \forall \varphi \in \mathrm{H}^1_D(\Omega), \tag{4.1}$$

$$b(u_j; v_j, \psi) \le \nu_j \|\psi\|_{\mathrm{H}^1(\Omega)} \qquad \forall \psi \in \mathrm{H}^1_c(\Omega) \cap \mathrm{L}^\infty(\Omega), \tag{4.2}$$

for some $\mu_j, \nu_j \in \mathbb{R}_{\ge 0}$, with μ_j, $\nu_j \to 0$ as $j \to \infty$. Suppose also that $((u_j, v_j))_{j=1}^{\infty}$ is a bounded sequence in $\mathrm{H}^1(\Omega) \times \mathrm{H}^1(\Omega)$.

Then, there exists a subsequence of $((u_j, v_j))_{j=1}^{\infty}$ (not relabelled) and $(u, v) \in \mathrm{H}^1_g(\Omega) \times \mathrm{H}^1_c(\Omega)$, with $0 \le v(x) \le 1$ a.e. in Ω, such that $u_j \to u$ strongly in $\mathrm{H}^1(\Omega)$ and $v_j \to v$ strongly in $\mathrm{H}^1(\Omega)$ as $j \to \infty$. Moreover, u and v satisfy

$$a(v; u, \varphi) = 0 \qquad \forall \varphi \in \mathrm{H}^1_D(\Omega), \tag{4.3}$$

$$b(u; v, \psi) = 0 \qquad \forall \psi \in \mathrm{H}^1_c(\Omega) \cap \mathrm{L}^\infty(\Omega); \tag{4.4}$$

that is, (u, v) is a critical point of I in $\mathrm{H}^1_g(\Omega) \times (\mathrm{H}^1_c(\Omega) \cap \mathrm{L}^\infty(\Omega))$.

Theorem 4.2 proves that the sequence $((u^n, v^n))_{n=1}^{\infty}$ computed by Algorithm 2′ (which is designed without a termination criterion) converges to a critical point of I and thus, subject to a justification of assumption (A), establishes the convergence of Algorithm 2′. To the best of our knowledge, this is the first convergence result for an adaptive finite element algorithm for a nonconvex minimization problem.

THEOREM 4.2. *Assume that Ω is an open bounded domain in $\mathbb{R}^N$. Let $((u_n, v_n))_{n=1}^{\infty} \subset \mathrm{H}^1_g(\Omega) \times \mathrm{H}^1_c(\Omega)$ be the sequence generated by Algorithm 2′ under assumption* (A).

Then, there exists a subsequence $((u_{n_j}, v_{n_j}))_{j=1}^{\infty}$ of $((u_n, v_n))_{n=1}^{\infty}$ and $(u, v) \in \mathrm{H}^1_g(\Omega) \times \mathrm{H}^1_c(\Omega)$, with $0 \le v(x) \le 1$ a.e. in Ω, such that $u_{n_j} \to u$ strongly in $\mathrm{H}^1(\Omega)$ and $v_{n_j} \to v$ strongly in $\mathrm{H}^1(\Omega)$ as $j \to \infty$. In addition, u and v satisfy

$$a(v; u, \varphi) = 0 \qquad \forall \varphi \in \mathrm{H}^1_D(\Omega), \tag{4.5}$$

$$b(u; v, \psi) = 0 \qquad \forall \psi \in \mathrm{H}^1_c(\Omega) \cap \mathrm{L}^\infty(\Omega); \tag{4.6}$$

that is, (u, v) is a critical point of I in $\mathrm{H}^1_g(\Omega) \times (\mathrm{H}^1_c(\Omega) \cap \mathrm{L}^\infty(\Omega))$.

Proof of Theorem 4.1.

Step 1. Existence of a convergent subsequence of $((u_j, v_j))_{j=1}^{\infty}$: The sequence $((u_j, v_j))_{j=1}^{\infty}$ is bounded in $\mathrm{H}^1(\Omega) \times \mathrm{H}^1(\Omega)$. Since $\mathrm{H}^1(\Omega)$ is a Hilbert space, there exists a subsequence of $((u_j, v_j))_{j=1}^{\infty}$ (not relabelled) such that

$$(u_j, v_j) \rightharpoonup (u, v) \qquad \text{in } \mathrm{H}^1(\Omega) \times \mathrm{H}^1(\Omega) \text{ as } j \to \infty.$$

As $\mathrm{H}^1_g(\Omega)$ is a convex and closed subset of $\mathrm{H}^1(\Omega)$, it is also weakly closed (cf. Proposition 2.5 on p. 35 of [6]). Hence, we have that $u \in \mathrm{H}^1_g(\Omega)$. Similarly, as the set $\mathrm{K} := \{w \in \mathrm{H}^1_c(\Omega) : 0 \le w(x) \le 1 \text{ a.e. } x \in \Omega\}$ is a convex closed subset of $\mathrm{H}^1(\Omega)$, and since $v_j \in \mathrm{K}$ for all $j \in \mathbb{N}$, it follows that $0 \le v(x) \le 1$ a.e. in Ω.

The compact embedding of $\mathrm{H}^1(\Omega)$ in $\mathrm{L}^2(\Omega)$ also implies that $u_j \to u$ and $v_j \to v$ strongly in $\mathrm{L}^2(\Omega)$ as $j \to \infty$.

Copyright © by SIAM. Unauthorized reproduction of this article is prohibited.

Step 2. $\lim_{j\to\infty}\int_\Omega |v-v_j|\,|\nabla w|^2\,\mathrm{d}x = 0$ for all $w \in \mathrm{H}^1(\Omega)$: (Recall that we have not relabelled the convergent subsequence.) This result will prove to be repeatedly useful in the subsequent analysis. Fix $w \in \mathrm{H}^1(\Omega)$, and let $(v_{j_k})_{k=1}^\infty$ be a subsequence of $(v_j)_{j=1}^\infty$ such that $\lim_{k\to\infty}\int_\Omega |v_{j_k}-v|\,|\nabla w|^2\,\mathrm{d}x = \limsup_{j\to\infty}\int_\Omega |v_j-v|\,|\nabla w|^2\,\mathrm{d}x$, and $v_{j_k}\to v$ a.e. in Ω. Using Lebesgue's dominated convergence theorem [38, section 5.2], we have $\lim_{k\to\infty}\int_\Omega |v_{j_k}-v|\,|\nabla w|^2\,\mathrm{d}x = 0$ and hence $\limsup_{j\to\infty}\int_\Omega |v_j-v|\,|\nabla w|^2\,\mathrm{d}x = 0$. It thus follows that $\lim_{j\to\infty}\int_\Omega |v_j-v|\,|\nabla w|^2\,\mathrm{d}x = 0$.

Step 3. $a(v;u,\varphi) = 0$ for all $\varphi \in \mathrm{H}^1_D(\Omega)$: Fixing $\varphi \in \mathrm{H}^1_D(\Omega)$, we have

$$\begin{aligned} a(v;u,\varphi) &= \int_\Omega (v^2+\eta)\nabla u\cdot\nabla\varphi\,\mathrm{d}x \\ &= \int_\Omega (v^2+\eta)\nabla(u-u_j)\cdot\nabla\varphi\,\mathrm{d}x \;+\; \int_\Omega (v_j^2+\eta)\nabla u_j\cdot\nabla\varphi\,\mathrm{d}x \\ &\quad+\; \int_\Omega (v^2-v_j^2)\nabla u_j\cdot\nabla\varphi\,\mathrm{d}x \\ &=: R_j + S_j + T_j. \end{aligned}$$

Our aim is to show that $R_j, S_j, T_j \to 0$ as $j\to\infty$. First, consider

$$R_j = \int_\Omega (v^2+\eta)\nabla\varphi\cdot\nabla(u-u_j)\,\mathrm{d}x.$$

We know that $(v^2+\eta)\nabla\varphi \in (\mathrm{L}^2(\Omega))^N$; so, by the weak convergence of $(\nabla u_j)_{j=1}^\infty$ to ∇u in $(\mathrm{L}^2(\Omega))^N$, we obtain that $R_j\to 0$ as $j\to\infty$.

Turning our attention to S_j, (4.1) implies that

$$|S_j| \;\le\; \mu_j\|\nabla\varphi\|_{\mathrm{L}^2(\Omega)} \to 0 \quad \text{as} \quad j\to\infty.$$

Finally, we estimate T_j by

$$\begin{aligned} |T_j| &\le \int_\Omega |v+v_j||v-v_j||\nabla u_j||\nabla\varphi|\,\mathrm{d}x \\ &\le 2\left(\int_\Omega |v-v_j|\,|\nabla\varphi|^2\,\mathrm{d}x\right)^{1/2}\|\nabla u_j\|_{\mathrm{L}^2(\Omega)}, \end{aligned}$$

where we used the fact $|v+v_j|\le 2$ and $|v-v_j|\le 1$. Since $(\nabla u_j)_{j=1}^\infty$ is bounded in $(\mathrm{L}^2(\Omega))^N$, and using Step 2 with $w=\varphi$, we have $T_j\to 0$ as $j\to\infty$. Thus we conclude that $a(v;u,\varphi)=0$ for all $\varphi\in\mathrm{H}^1_D(\Omega)$.

Step 4. $\nabla u_j\to\nabla u$ strongly in $(\mathrm{L}^2(\Omega))^N$: Note that

$$\begin{aligned} \eta\|\nabla u-\nabla u_j\|^2_{\mathrm{L}^2(\Omega)} &\le \int_\Omega (v_j^2+\eta)\nabla(u-u_j)\cdot\nabla(u-u_j)\,\mathrm{d}x \\ &= -\int_\Omega (v_j^2+\eta)\nabla u_j\cdot\nabla(u-u_j)\,\mathrm{d}x + \int_\Omega (v_j^2+\eta)\nabla u\cdot\nabla(u-u_j)\,\mathrm{d}x \\ &\le \mu_j\|\nabla(u-u_j)\|_{\mathrm{L}^2(\Omega)} + \int_\Omega (v_j^2+\eta)\nabla u\cdot\nabla(u-u_j)\,\mathrm{d}x. \end{aligned}$$

Since $u-u_j\in\mathrm{H}^1_D(\Omega)$, we have $a(v;u,u-u_j)=0$, and it follows that

$$\begin{aligned} \eta\|\nabla u-\nabla u_j\|^2_{\mathrm{L}^2(\Omega)} &\le \mu_j\|\nabla(u-u_j)\|_{\mathrm{L}^2(\Omega)} + \int_\Omega (v_j^2-v^2)\nabla u\cdot\nabla(u-u_j)\,\mathrm{d}x \\ &\le \mu_j\|\nabla(u-u_j)\|_{\mathrm{L}^2(\Omega)} + \|(v_j^2-v^2)\nabla u\|_{\mathrm{L}^2(\Omega)}\|\nabla(u-u_j)\|_{\mathrm{L}^2(\Omega)}. \end{aligned}$$

Copyright © by SIAM. Unauthorized reproduction of this article is prohibited.

Dividing by $\|\nabla u - \nabla u_j\|$ and using the fact that $|v_j^2 - v^2|^2 \leq 4|v_j - v|^2 \leq 4|v_j - v|$, we obtain

$$\eta\|\nabla u - \nabla u_j\|_{\mathrm{L}^2(\Omega)} \leq \mu_j + \|(v_j^2 - v^2)\nabla u\|_{\mathrm{L}^2(\Omega)} \leq \mu_j + 2\left(\int_\Omega |v_j - v|\,|\nabla u|^2\,\mathrm{d}x\right)^{1/2}.$$

Since $\mu_j \to 0$ as $j \to \infty$, and using Step 2, we deduce that $\lim_{j\to\infty} \|\nabla u - \nabla u_j\|_{\mathrm{L}^2(\Omega)} = 0$.

Step 5. $b(u; v, \psi) = 0$ for all $\psi \in \mathrm{H}^1_c(\Omega) \cap \mathrm{L}^\infty(\Omega)$: Fixing $\psi \in \mathrm{H}^1_c(\Omega) \cap \mathrm{L}^\infty(\Omega)$, we have

$$\begin{aligned} b(u; v, \psi) &= \int_\Omega \left[(|\nabla u|^2 + \alpha)v\psi - \alpha\psi + \varepsilon\nabla v \cdot \nabla\psi\right]\mathrm{d}x \\ &= \int_\Omega \left[(|\nabla u|^2 + \alpha)(v - v_j)\psi + \varepsilon\nabla(v - v_j) \cdot \nabla\psi\right]\mathrm{d}x \\ &\quad + \int_\Omega \left[(|\nabla u_j|^2 + \alpha)v_j\psi - \alpha\psi + \varepsilon\nabla v_j \cdot \nabla\psi\right]\mathrm{d}x \\ &\quad + \int_\Omega \left[(|\nabla u|^2 - |\nabla u_j|^2)v_j\psi\right]\mathrm{d}x \\ &=: R_j + S_j + T_j. \end{aligned}$$

We can estimate R_j by

$$\begin{aligned} |R_j| &\leq \left|\int_\Omega |\nabla u|^2(v - v_j)\psi\,\mathrm{d}x\right| + \alpha\|v - v_j\|_{\mathrm{L}^2(\Omega)}\|\psi\|_{\mathrm{L}^2(\Omega)} \\ &\quad + \varepsilon\left|\int_\Omega \nabla(v - v_j) \cdot \nabla\psi\,\mathrm{d}x\right| \\ &\leq \|\psi\|_{\mathrm{L}^\infty(\Omega)}\int_\Omega |\nabla u|^2|v - v_j|\,\mathrm{d}x + \alpha\|v - v_j\|_{\mathrm{L}^2(\Omega)}\|\psi\|_{\mathrm{L}^2(\Omega)} \\ &\quad + \varepsilon\left|\int_\Omega \nabla(v - v_j) \cdot \nabla\psi\,\mathrm{d}x\right|. \end{aligned}$$

Since $v_j \to v$ in $\mathrm{L}^2(\Omega)$, $\nabla v_j \rightharpoonup \nabla v$ in $(\mathrm{L}^2(\Omega))^N$, and using Step 2 with $w = u$, we deduce that $R_j \to 0$ as $j \to \infty$.

Now, from (4.2) we know that $|S_j| \leq \nu_j\|\psi\|_{\mathrm{H}^1(\Omega)} \to 0$, and therefore $S_j \to 0$ as $j \to \infty$.

Last, we estimate T_j by

$$\begin{aligned} |T_j| &= \left|\int_\Omega \left[(|\nabla u|^2 - |\nabla u_j|^2)v_j\psi\right]\mathrm{d}x\right| \\ &\leq \|\psi\|_{\mathrm{L}^\infty(\Omega)}\int_\Omega |\nabla(u - u_j)||\nabla(u + u_j)|\,\mathrm{d}x \\ &\leq \|\psi\|_{\mathrm{L}^\infty(\Omega)}\|\nabla(u - u_j)\|_{\mathrm{L}^2(\Omega)}\|\nabla(u + u_j)\|_{\mathrm{L}^2(\Omega)}. \end{aligned}$$

Since $\nabla u_j \to \nabla u$ in $(\mathrm{L}^2(\Omega))^N$, we obtain $T_j \to 0$ as $j \to \infty$. Hence $b(u; v, \psi) = 0$ for all $\psi \in \mathrm{H}^1_c(\Omega) \cap \mathrm{L}^\infty(\Omega)$.

Copyright © by SIAM. Unauthorized reproduction of this article is prohibited.

Step 6. $\nabla v_j \to \nabla v$ strongly in $(\mathrm{L}^2(\Omega))^N$: Observe that

$$\begin{aligned}
&\varepsilon\|\nabla v - \nabla v_j\|^2_{\mathrm{L}^2(\Omega)}\\
&\quad\le \int_\Omega \big[(|\nabla u|^2+\alpha)|v-v_j|^2 + \varepsilon(\nabla v - \nabla v_j)\cdot(\nabla v - \nabla v_j)\big]\,\mathrm{d}x\\
&\quad= -\int_\Omega \big[(|\nabla u|^2+\alpha)v_j(v-v_j) + \varepsilon\nabla v_j\cdot\nabla(v-v_j) - \alpha(v-v_j)\big]\,\mathrm{d}x\\
&\qquad+\int_\Omega \big[(|\nabla u|^2+\alpha)v(v-v_j) + \varepsilon\nabla v\cdot\nabla(v-v_j) - \alpha(v-v_j)\big]\,\mathrm{d}x\\
&\quad= -b(u_j; v_j, v-v_j) + \int_\Omega (|\nabla u_j|^2 - |\nabla u|^2)v_j(v-v_j)\,\mathrm{d}x + b(u; v, v-v_j).
\end{aligned}$$

We have already shown that $b(u; v, v-v_j) = 0$, and hence

$$\begin{aligned}
\varepsilon\|\nabla v - \nabla v_j\|^2_{\mathrm{L}^2(\Omega)} &\le |b(u_j; v_j, v-v_j)| + \int_\Omega |\nabla u_j + \nabla u||\nabla u_j - \nabla u||v_j||v-v_j|\,\mathrm{d}x\\
&\le \nu_j\|v-v_j\|_{\mathrm{H}^1(\Omega)} + \|\nabla u + \nabla u_j\|_{\mathrm{L}^2(\Omega)}\|\nabla u_j - \nabla u\|_{\mathrm{L}^2(\Omega)}.
\end{aligned}$$

Since $\nu_j \to 0$, $\nabla u_j \to \nabla u$ in $(\mathrm{L}^2(\Omega))^N$, and since $(\|\nabla u + \nabla u_j\|_{\mathrm{L}^2(\Omega)})_{j=1}^\infty$ and $(\|v - v_j\|_{\mathrm{H}^1(\Omega)})_{j=1}^\infty$ are bounded, we deduce that $\nabla v_j \to \nabla v$ in $(\mathrm{L}^2(\Omega))^N$ as $j\to\infty$, which completes the proof of the theorem. ∎

Proof of Theorem 4.2.

Step 1. Existence of convergent subsequences of $((u_n, v_n))_{n=1}^\infty$: Since $((u_n, v_n))_{n=1}^\infty$ is a bounded sequence in $\mathrm{H}^1_g(\Omega)\times\mathrm{H}^1_c(\Omega)$, it follows analogously to Step 1 in the proof of Theorem 4.1 that there exists a subsequence $((u_{n_j}, v_{n_j}))_{j=1}^\infty$ of $((u_n, v_n))_{n=1}^\infty$ such that

$$(u_{n_j}, v_{n_j}) \rightharpoonup (u, v) \qquad \text{in } \mathrm{H}^1(\Omega)\times\mathrm{H}^1(\Omega) \text{ as } j\to\infty$$

for some $u\in\mathrm{H}^1_g(\Omega)$ and $v\in\mathrm{H}^1_c(\Omega)$, with $0\le v(x)\le 1$ a.e. in Ω. It will be seen that careful labelling of the subsequence is vital in the proof.

Upon extracting a further subsequence, we may assume, without loss of generality, that $v_{n_j+1} \rightharpoonup v'$ weakly in $\mathrm{H}^1(\Omega)$ for some $v'\in\mathrm{H}^1(\Omega)$.

Step 2. $a(v; u, \varphi) = 0$ for all $\varphi\in\mathrm{H}^1_D(\Omega)$: By definition of $((u_{n_j}, v_{n_j}))_{j=1}^\infty$, we have

$$a(v_{n_j}; u_{n_j}, \varphi) \le \mu_{n_j}\|\nabla\varphi\|_{\mathrm{L}^2(\Omega)} \qquad \forall j\in\mathbb{N} \text{ and } \forall\varphi\in\mathrm{H}^1_D(\Omega),$$

with $\mu_{n_j}\to 0$ as $j\to\infty$. It follows analogously to Steps 3 and 4 of the proof of Theorem 4.1 that

$$a(v; u, \varphi) = 0 \qquad \forall\varphi\in\mathrm{H}^1_D(\Omega)$$

and also that $\nabla u_{n_j}\to\nabla u$ in $(\mathrm{L}^2(\Omega))^N$ as $j\to\infty$.

Step 3. Strong convergence of $(v_{n_j+1})_{j=1}^\infty$: By the compact embedding of $\mathrm{H}^1(\Omega)$ in $\mathrm{L}^2(\Omega)$, it follows that $v_{n_j+1}\to v'$ strongly in $\mathrm{L}^2(\Omega)$. To obtain strong convergence in $\mathrm{H}^1(\Omega)$, note that the sequence $((u_{n_j}, v_{n_j+1}))_{j=1}^\infty$ satisfies

$$b(u_{n_j}; v_{n_j+1}, \psi) \le \nu_{n_j}\|\nabla\psi\|_{\mathrm{L}^2(\Omega)} \qquad \forall j\in\mathbb{N} \text{ and } \forall\psi\in\mathrm{H}^1_c(\Omega).$$

Taking $\psi = (v_{n_{j+1}} - v')\in\mathrm{H}^1_c(\Omega)$, it follows that

$$\begin{aligned}
\nu_{n_j}\|\nabla\psi\|_{\mathrm{L}^2(\Omega)} \ge \int_\Omega v_{n_j+1}(v_{n_j+1}-v')\,|\nabla u_{n_j}|^2\,\mathrm{d}x + \alpha\int_\Omega (1-v_{n_j+1})(v_{n_j+1}-v')\,\mathrm{d}x\\
+\varepsilon\int_\Omega \nabla v_{n_j+1}\cdot(\nabla v_{n_j+1} - \nabla v')\,\mathrm{d}x,
\end{aligned}$$

Copyright © by SIAM. Unauthorized reproduction of this article is prohibited.

and therefore

$$\begin{aligned}
\varepsilon \int_\Omega |\nabla v_{n_j+1}|^2 \,\mathrm{d}x
&\leq \int_\Omega v_{n_j+1}(v' - v_{n_j+1})|\nabla u|^2 \,\mathrm{d}x + \int_\Omega v_{n_j+1}(v' - v_{n_j+1})(|\nabla u_{n_j}|^2 - |\nabla u|^2)\,\mathrm{d}x \\
&\quad + \alpha \int_\Omega (1 - v_{n_j+1})(v' - v_{n_j+1})\,\mathrm{d}x + \varepsilon \int_\Omega \nabla v_{n_j+1} \cdot \nabla v' \,\mathrm{d}x \\
&\quad + \nu_{n_j} \|\nabla \psi\|_{\mathrm{L}^2(\Omega)}, \\
&\leq \int_\Omega |v' - v_{n_j+1}|\, |\nabla u|^2 \,\mathrm{d}x + \|\nabla u_{n_j} - \nabla u\|_{\mathrm{L}^2(\Omega)} \|\nabla u_{n_j} + \nabla u\|_{\mathrm{L}^2(\Omega)} \\
&\quad + \alpha \int_\Omega |v' - v_{n_j+1}|\,\mathrm{d}x + \varepsilon \left| \int_\Omega \nabla v_{n_j+1} \cdot \nabla v' \,\mathrm{d}x \right| + \nu_{n_j} \|\nabla \psi\|_{\mathrm{L}^2(\Omega)}.
\end{aligned}$$

Letting $j \to \infty$, we obtain

$$\limsup_{j\to\infty} \varepsilon \int_\Omega |\nabla v_{n_j+1}|^2 \leq \varepsilon \int_\Omega |\nabla v'|^2 \,\mathrm{d}x.$$

Using the weak lower semicontinuity of the L^2-norm, we conclude that

$$\int_\Omega |\nabla v'|^2 \leq \liminf_{j\to\infty} \int_\Omega |\nabla v_{n_j+1}|^2 \,\mathrm{d}x \leq \limsup_{j\to\infty} \int_\Omega |\nabla v_{n_j+1}|^2 \,\mathrm{d}x \leq \int_\Omega |\nabla v'|^2 \,\mathrm{d}x.$$

Thus we deduce that $\|\nabla v_{n_j+1}\|_{\mathrm{L}^2(\Omega)} \to \|\nabla v'\|_{\mathrm{L}^2(\Omega)}$, which, together with weak convergence, implies the strong convergence of $v_{n_{j+1}}$ to v' in $\mathrm{H}^1(\Omega)$ as $j \to \infty$.

Step 4. $v = v'$; $b(u; v, \psi) = 0$ for all $\psi \in \mathrm{H}^1_c(\Omega) \cap \mathrm{L}^\infty(\Omega)$: Note that the sequence $((u_{n_j}, v_{n_j+1}))_{j=1}^\infty$ satisfies

$$b(u_{n_j}; v_{n_j+1}, \psi) \leq \nu_{n_j} \|\nabla \psi\|_{\mathrm{L}^2(\Omega)} \qquad \forall j \in \mathbb{N} \text{ and } \forall \psi \in \mathrm{H}^1_c(\Omega) \cap \mathrm{L}^\infty(\Omega).$$

Letting $j \to \infty$, it follows analogously to Step 5 in the proof of Theorem 4.1 that

$$b(u; v', \psi) = 0 \qquad \forall \psi \in \mathrm{H}^1_c(\Omega) \cap \mathrm{L}^\infty(\Omega),$$

and we are left to show that $v = v'$.

Using the weak lower semicontinuity of I, together with property 6 of Lemma 3.3, it follows that

$$I(u, v) \leq \liminf_{j\to\infty} I(u_{n_{j+1}}, v_{n_{j+1}}) \leq \lim_{j\to\infty} I(u_{n_j}, v_{n_j+1}) = I(u, v').$$

Since v' is a critical point of the strictly convex map $v \mapsto I(u, v)$, v' is its unique minimizer. Since $I(u, v) = I(u, v')$, it follows that $v = v'$ and hence (u, v) is a critical point of I. ∎

5. Computational examples. The purpose of this section is to present some preliminary numerical results for the adaptive algorithms proposed in section 3.2. We will consider two examples chosen to address some of the relevant questions concerning the method.

Copyright © by SIAM. Unauthorized reproduction of this article is prohibited.

5.1. An example of a straight crack in a two-dimensional domain. We take Ω to be the rectangular domain $(0,2) \times (0,2.2)$ containing a slit along $\{1\} \times [1.5, 2.2]$. This is shown in Figure 5.1, where the shaded part $\big((0,1) \cup (1,2)\big) \times (2, 2.2)$ is Ω_D. The incremental antiplane displacement $g(x,t)$ is given as follows:

$$g(x,t) = \begin{cases} -t & \text{on } (0,1) \times (2, 2.2), \\ t & \text{on } (1,2) \times (2, 2.2), \end{cases}$$

where $t = 0.01$s for s $= 0, 1, \ldots, 140$. We fix $\varepsilon = 0.02$, $\eta = 1 \times 10^{-5}$, $\texttt{VTOL} = 1 \times 10^{-3}$, $\texttt{REFTOL} = 0.05$, $\texttt{CRTOL} = 1 \times 10^{-4}$, and $\theta = 0.3$. At each time step, the initial crack field v is taken to be the final computed v from the previous time step, with the exception of the first time step, where it is taken to be $v \equiv 1$. In the implementation, we do not enforce condition (2.2).

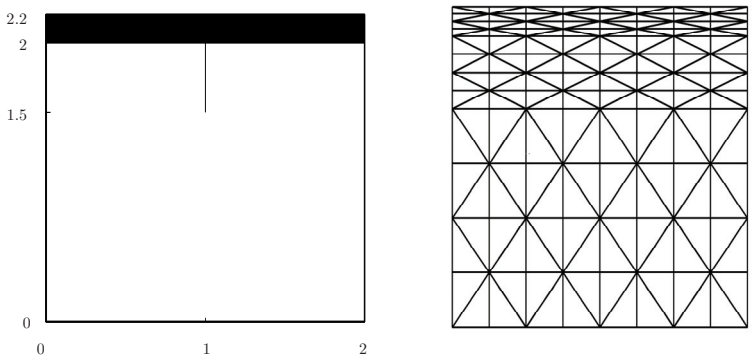

(a) Domain (b) Initial mesh

FIG. 5.1. *The computational domain for the straight crack example.*

We compute the evolution of u and v using Algorithms 1 and 2. Figure 5.2 shows the resulting crack field variable v and mesh at the final time, together with the change in bulk, surface, and total energy over time. Both algorithms compute a very similar evolution; the body remains unfractured until time $t \sim 0.35$, when a period of continuous slow crack growth begins. This ends at time $t = 1.28$, when *failure* occurs, in which the crack length rapidly increases, splitting the body into two pieces. The sudden decrease in the total energy at this time reveals that both algorithms have computed local minimizers of the energy.

In computing the evolution of the crack, those elements of the initial mesh located near the crack path are refined the most. However, it should also be noted that each element of the initial mesh is refined at least once, since it is necessary to resolve the elastic solution, as well as the crack, to the desired accuracy. We also observe that, although the crack grows relatively straight for both algorithms, there is a slight deviation from the line $x = 1$.

The total number of elements in the final mesh computed by Algorithms 1 and 2 are 300658 and 507539, respectively. In both meshes, the smallest and largest elements have diameters of orders 10^{-5} and 10^{-1}, respectively. The total number of linear systems solved by Algorithms 1 and 2 are 10556 and 8018, respectively. It is observed

Copyright © by SIAM. Unauthorized reproduction of this article is prohibited.

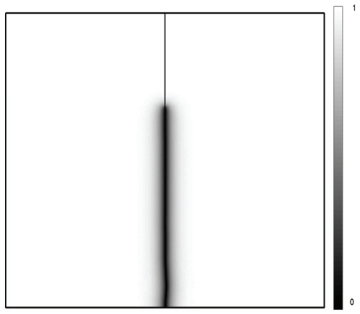

(a) The final v-field computed by Algorithm 1

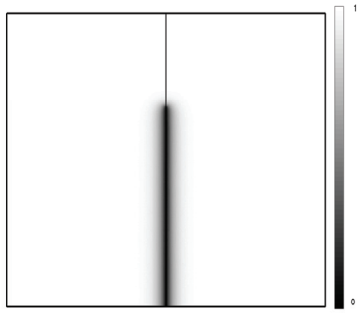

(b) The final v-field computed by Algorithm 2

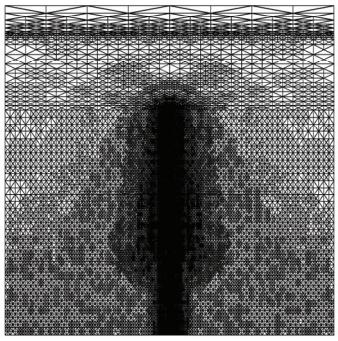

(c) The final mesh computed by Algorithm 1

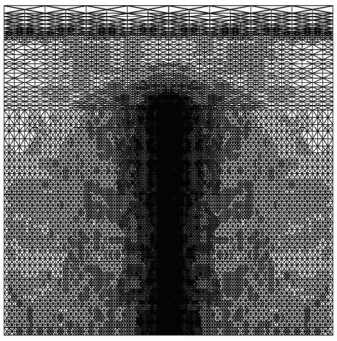

(d) The final mesh computed by Algorithm 2

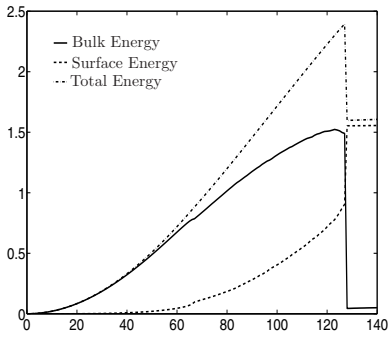

(e) The energy computed by Algorithm 1

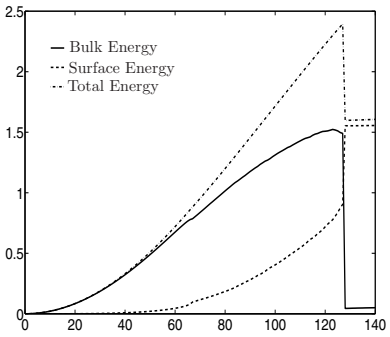

(f) The energy computed by Algorithm 2

FIG. 5.2. *The final crack path, final mesh, and evolution of the energy computed by Algorithms* 1 *and* 2. *The number of elements in the meshes are* 300658 *and* 507539, *respectively. The total number of linear systems solved by the two algorithms are* 10556 *and* 8018, *respectively.*

Copyright © by SIAM. Unauthorized reproduction of this article is prohibited.

that, at each time step, Algorithm 1 generally involves more alternate minimization steps than Algorithm 2; however, Algorithm 2 requires a larger number of refinement iterations.

5.2. An example of a curved crack in a two-dimensional domain. We now consider the case of a curved crack occurring in a two-dimensional domain. In this example, we focus on Algorithm 2 with the aim of investigating how the computational results respond to changes in ε and `REFTOL`.

Take Ω to be the two-dimensional rectangular domain $(0,2)\times(0,2.2)$, containing a slit along $\{1\}\times[1.5,2.2]$, and a circular hole with center $(0.3,0.3)$, radius 0.2. This is shown in Figure 5.3, where the shaded part $\big((0,1)\cup(1,2)\big)\times(2,2.2)$ is Ω_D. The incremental antiplane displacement $g(x,t)$ is given as follows:

$$g(x,t)=\begin{cases} -t & \text{on } (0,1)\times(2,2.2),\\ t & \text{on } (1,2)\times(2,2.2),\end{cases}$$

where $t = 0.01\text{s}$ for $\text{s} = 0,1,\ldots,140$. In all subsequent experiments, we fix $\eta = 1\times10^{-5}$, `VTOL` $= 1\times10^{-3}$, `CRTOL` $= 1\times10^{-4}$, and $\theta = 0.3$. The initial triangulation of the domain, shown in Figure 5.3, is generated using the software package Triangle [32, 33]. The initial crack field v is chosen as in the example of a straight crack in section 5.1.

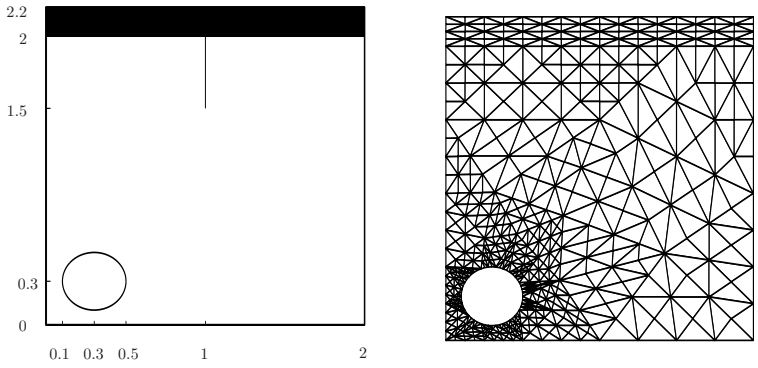

(a) Domain (b) Initial mesh

FIG. 5.3. *The computational domain for the curved crack example.*

We first use Algorithm 2 to compute the evolution of the crack with $\varepsilon = 0.02$ and `REFTOL` $= 0.05$. Figure 5.4 shows the crack field variable v and the mesh at the final time step, together with the change in bulk, surface, and total energies over time. The body first remains unfractured until time $t \sim 0.25$, when the applied displacement becomes sufficiently large to initiate a crack at the slit tip. A period of slow continuous crack growth then follows until failure occurs at time $t = 1.24$. Once again the sharp decrease in the total energy at this time reveals that a local minimizer of the energy has been computed by the algorithm.

It is important to consider how the choice of ε and `REFTOL` affects the evolution of the crack. The computed crack path will converge to some limiting curve as ε and `REFTOL` tend to zero; however, if these parameters are not chosen sufficiently small, then it is possible to compute a wide variation of crack paths. This is demonstrated

Copyright © by SIAM. Unauthorized reproduction of this article is prohibited.

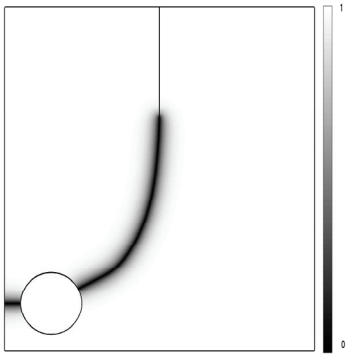

(a) Crack path: plot of v

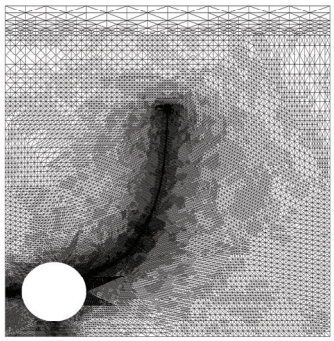

(b) Final mesh

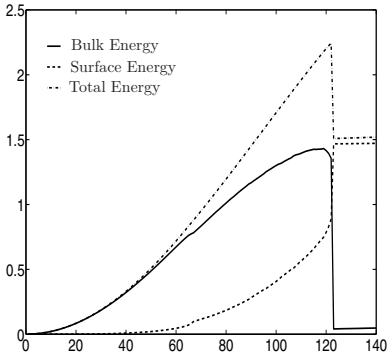

(c) Bulk and surface energy

FIG. 5.4. *The evolution of the body computed by Algorithm* 2 *for* $\varepsilon = 0.02$ *and* `REFTOL` $= 0.05$. *The number of elements in the final mesh is* 429116*, with the smallest and largest elements having diameters of order* 10^{-4} *and* 10^{-1}*, respectively.*

in Figure 5.5, which shows the final crack path computed for a range of parameter values using Algorithm 2.

There are two separate issues highlighted by Figure 5.5. The first is a numerical matter; the subfigures show that for each fixed value of ε a sufficiently small refinement tolerance must be used to ensure that an accurate crack path is computed. The second issue is one of modeling; the significant difference in the crack paths (d) and (h) shows the necessity of using a sufficiently small value of ε. Consequently, it is important to verify a computed crack path by comparing it with one computed using a smaller value of ε and `REFTOL`. This is clearly more easily achievable using an adaptively refined mesh rather than a uniform mesh.

Thus far we have considered only Algorithm 2. We now compare the results of Algorithms 1 and 2 with the choice of parameters $\varepsilon = 0.02$ and `REFTOL` $= 0.05$. A comparison by eye shows that the final crack paths computed by Algorithms 1 and 2 are similar; see Figure 5.6. The failure time for Algorithm 1 is at $t = 1.25$, one time

Copyright © by SIAM. Unauthorized reproduction of this article is prohibited.

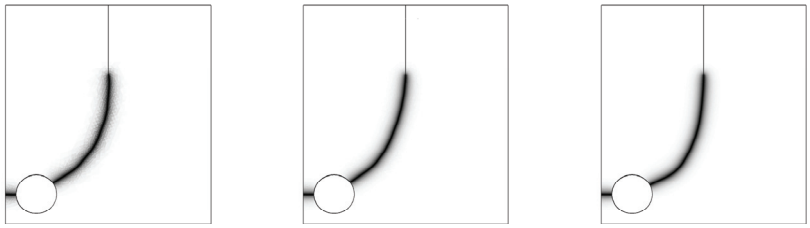

(a) $\varepsilon = 0.02$, REFTOL $= 0.3$ (b) $\varepsilon = 0.02$, REFTOL $= 0.1$ (c) $\varepsilon = 0.02$, REFTOL $= 0.05$

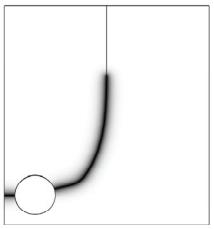

(d) $\varepsilon = 0.02$, REFTOL $= 0.03$

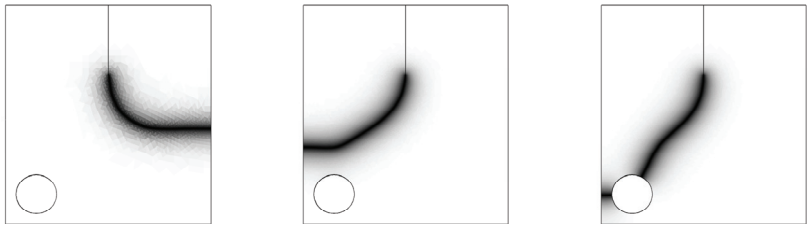

(e) $\varepsilon = 0.05$, REFTOL $= 0.3$ (f) $\varepsilon = 0.05$, REFTOL $= 0.1$ (g) $\varepsilon = 0.05$, REFTOL $= 0.05$

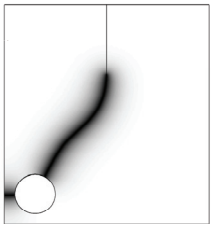

(h) $\varepsilon = 0.05$, REFTOL $= 0.03$

FIG. 5.5. *A comparison of the final crack path computed by Algorithm* 2 *for different values of* ε *and* REFTOL.

Copyright © by SIAM. Unauthorized reproduction of this article is prohibited.

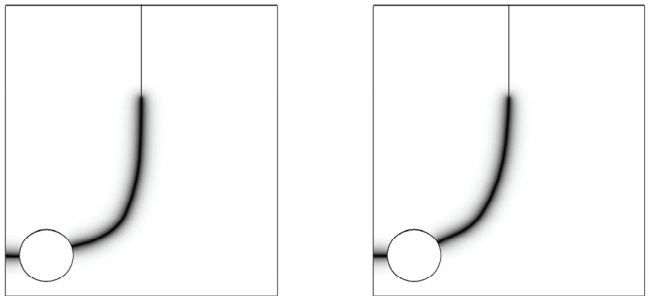

(a) Crack path for Algorithm 1 (b) Crack path for Algorithm 2

FIG. 5.6. *The final crack path computed using Algorithms* 1 *and* 2 *for* $\varepsilon = 0.02$ *and* `REFTOL` $= 0.05$. *The total number of elements in the final mesh for Algorithms* 1 *and* 2 *are* 256604 *and* 429116*, respectively, whilst the total number of linear systems solved by each algorithm are* 9126 *and* 6510*, respectively.*

step later than that of Algorithm 2. The total number of linear systems solved by Algorithm 1 is greater than that for Algorithm 2, whilst the number of elements in the final mesh for Algorithm 1 is fewer than that for Algorithm 2.

In general, we comment that even with the use of adaptive mesh refinement the computations are fairly demanding. To simulate more involved examples, it would be beneficial to improve the efficiency of the algorithms, for example, by using more powerful linear solvers or introducing mesh coarsening.

Remark 7. We note that, despite the fact many of the meshes generated by Algorithms 1 and 2 fail to satisfy condition (2.2), in all the computations we observe that $0 \leq v_h(x) \leq 1$ for all $x \in \Omega$.

6. Conclusion. We have presented two adaptive algorithms for computing finite element approximations of local minimizers of the Ambrosio–Tortorelli functional. In this paper, we have focused primarily on proving convergence results for the two algorithms. We have been able to show that, provided the associated residuals converge to zero, both algorithms generate a sequence of numerical solutions that converge to a critical point of I (as the termination tolerances tend to zero). Our preliminary computational results demonstrate the potential of using this method. In particular, we believe that the algorithms enable us to accurately and reliably compute the evolution of crack paths using considerably fewer elements compared to simulations with uniform meshes. However, we have observed that the crack path can be sensitive to the choice of the parameters in the adaptive algorithm. We will investigate this further through more extensive testing of the algorithms in future work.

We believe that the results presented are easily extendable to the cases of planar and three-dimensional elasticity. We are currently working on extending the theory and implementation to these models.

REFERENCES

[1] L. AMBROSIO, *A compactness theorem for a new class of functions of bounded variation*, Boll. Un. Mat. Ital. B (7), 3 (1989), pp. 857–881.

Copyright © by SIAM. Unauthorized reproduction of this article is prohibited.

[2] L. Ambrosio, *Existence theory for a new class of variational problems*, Arch. Rational Mech. Anal., 111 (1990), pp. 291–322.
[3] L. Ambrosio, N. Fusco, and D. Pallara, *Functions of Bounded Variation and Free Discontinuity Problems*, Oxford University Press, New York, 2000.
[4] L. Ambrosio and V. M. Tortorelli, *Approximation of functionals depending on jumps by elliptic functionals via* Γ*-convergence*, Comm. Pure Appl. Math., 43 (1990), pp. 999–1036.
[5] L. Ambrosio and V. M. Tortorelli, *On the approximation of free discontinuity problems*, Boll. Un. Mat. Ital. B (7), 6 (1992), pp. 105–123.
[6] V. Barbu and T. Precopeanu, *Convexity and Optimization in Banach Spaces*, D. Reidel, Dordrecht, The Netherlands, 1986.
[7] G. Bellettini and A. Coscia, *Discrete approximation of a free discontinuity problem*, Numer. Funct. Anal. Optim., 15 (1994), pp. 201–224.
[8] B. Bourdin, *Numerical implementation of the variational formulation for quasi-static brittle fracture*, Interfaces Free Bound., 9 (2007), pp. 411–430.
[9] B. Bourdin, *The variational formulation of brittle fracture: Numerical implementation and extensions*, in IUTAM Symposium on Discretization Methods for Evolving Discontinuities, Springer-Verlag, Dordrecht, The Netherlands, 2007, pp. 381–393.
[10] B. Bourdin and A. Chambolle, *Implementation of an adaptive finite element approximation of the Mumford-Shah functional*, Numer. Math., 85 (2000), pp. 609–646.
[11] B. Bourdin, G. A. Francfort, and J.-J. Marigo, *Numerical experiments in revisited brittle fracture*, J. Mech. Phys. Solids, 48 (2000), pp. 797–826.
[12] A. Braides, Γ*-Convergence for Beginners*, Oxford Lecture Ser. Math. Appl. 22, Oxford University Press, Oxford, UK, 2002.
[13] S. C. Brenner and L. R. Scott, *The Mathematical Theory of Finite Element Methods*, 2nd ed., Springer-Verlag, New York, 1994.
[14] S. Burke, C. Ortner, and E. Süli, *An Adaptive Finite Element Approximation of the Generalised Ambrosio–Tortorelli Functional*, manuscript, 2010.
[15] J. M. Cascon, C. Kreuzer, R. H. Nochetto, and K. G. Siebert, *Quasi-optimal convergence rate for an adaptive finite element method*, SIAM J. Numer. Anal., 46 (2008), pp. 2524–2550.
[16] A. Chambolle and G. Dal Maso, *Discrete approximation of the Mumford-Shah functional in dimension two*, M2AN Math. Model. Numer. Anal., 33 (1999), pp. 651–672.
[17] P. G. Ciarlet and P.-A. Raviart, *Maximum principle and uniform convergence for the finite element method*, Comput. Methods Appl. Mech. Engrg., 2 (1973), pp. 17–31.
[18] G. Dal Maso, G. A. Francfort, and R. Toader, *Quasistatic crack growth in nonlinear elasticity*, Arch. Ration. Mech. Anal., 176 (2005), pp. 165–225.
[19] G. Dal Maso and R. Toader, *A model for the quasi-static growth of brittle fractures: Existence and approximation results*, Arch. Ration. Mech. Anal., 162 (2002), pp. 101–135.
[20] E. De Giorgi, M. Carriero, and A. Leaci, *Existence theorem for a minimum problem with free discontinuity set*, Arch. Rational Mech. Anal., 108 (1989), pp. 195–218.
[21] W. Dörfler, *A convergent adaptive algorithm for Poisson's equation*, SIAM J. Numer. Anal., 33 (1996), pp. 1106–1124.
[22] L. C. Evans and R. F. Gariepy, *Measure Theory and Fine Properties of Functions*, Stud. Adv. Math., CRC Press, Boca Raton, FL, 1992.
[23] M. Focardi, *On the variational approach of free discontinuity problems in the vectorial case*, Math. Models Methods Appl. Sci., 11 (2001), pp. 663–684.
[24] G. A. Francfort and C. J. Larsen, *Existence and convergence for quasi-static evolution in brittle fracture*, Comm. Pure Appl. Math., 56 (2003), pp. 1465–1500.
[25] G. A. Francfort and J.-J. Marigo, *Revisiting brittle fracture as an energy minimization problem*, J. Mech. Phys. Solids, 46 (1998), pp. 1319–1342.
[26] A. Giacomini, *Ambrosio-Tortorelli approximation of quasi-static evolution of brittle fractures*, Calc. Var. Partial Differential Equations, 22 (2005), pp. 129–172.
[27] A. A. Griffith, *The phenomena of rupture and flow in solids*, Phil. Trans. Roy. Soc. London Ser. A, 221 (1921), pp. 163–198.
[28] S. Korotov, M. Křížek, and P. Neittaanmäki, *Weakened acute type condition for tetrahedral triangulations and the discrete maximum principle*, Math. Comp., 70 (2001), pp. 107–119.
[29] W. Mitchell, *A comparison of adaptive refinement techniques for elliptic problems*, ACM Trans. Math. Software, 15 (1989), pp. 326–247.
[30] D. Mumford and J. Shah, *Optimal approximation by piecewise smooth functions and associated variational problems*, Comm. Pure Appl. Math., 42 (1989), pp. 577–685.
[31] M. Negri and M. Paolini, *Numerical minimization of the Mumford-Shah functional*, Calcolo, 38 (2001), pp. 67–84.

Copyright © by SIAM. Unauthorized reproduction of this article is prohibited.

[32] J. R. Shewchuk, *Triangle: Engineering a 2D quality mesh generator and Delaunay triangulator*, in Applied Computational Geometry: Towards Geometric Engineering, Lecture Notes in Comput. Sci. 1148, M. C. Lin and D. Manocha, eds., Springer-Verlag, Berlin, 1996, pp. 203–222.
[33] J. R. Shewchuk, *Delaunay refinement algorithms for triangular mesh generation*, Comput. Geom., 22 (2002), pp. 21–74.
[34] G. Strang and G. J. Fix, *An Analysis of the Finite Element Method*, Prentice–Hall, Englewood Cliffs, NJ, 1973.
[35] V. Thomée, *Galerkin Finite Element Methods for Parabolic Problems*, Lecture Notes in Math. 1054, Springer-Verlag, Berlin, 1984.
[36] R. Verfürth, *A Review of A Posteriori Error Estimation and Adaptive Mesh-Refinement Techniques*, Wiley-Teubner, Chichester, Stuttgart, 1996.
[37] R. Verfürth, *Error estimates for some quasi-interpolation operators*, M2AN Math. Model. Numer. Anal., 33 (1999), pp. 695–713.
[38] A. J. Weir, *Lebesgue Integration and Measure*, Cambridge University Press, London, New York, 1973.

Copyright © by SIAM. Unauthorized reproduction of this article is prohibited.